CHARLES UNIVERSITY

Faculty of Pharmacy in Hradec Králové

Department of Pharmaceutical Technology

Study of the effect of biomolecules on the solubility of poorly soluble drugs

Diploma thesis

Fatemeh Kheirabadi
Hradec Králové
2023

Supervisor: Dr.Ondrej Holas , Ph.D.
Consultant: Professor Anette Mullertz

I hereby confirm that this thesis is my original copyrighted work. I compiled and elaborated it independently in my own words and in accordance with copyright. All resourcesand literature I used are indexed in the bibliography and properly cited. The thesis was not written and intended as misuse for obtaining the same or different academic degree.

Date and signature: 20.08.2023

Preface

This thesis serves as the final requirement for me to obtain a master's degree in Pharmacy from the Faculty of Pharmacy at Charles University in Hradec Kralove. Under the supervision of Dr. Ondrej Holas, Ph.D., the duration of this thesis extended from October 2022 to May 2023, and it accounts for 31 ECTS points

The data collection and scientific research for this thesis were carried out at the Research Group for Physiological Pharmaceutics, which is located within the Department of Pharmacy at the Faculty of Health and Medical Sciences at the University of Copenhagen. The experimental material used in the study consisted of porcine intestines obtained from the Department of Experimental Medicine at the University of Copenhagen, Denmark. The laboratory work was supervised by Professor Anette Müllertz, with co-supervision by PhD fellow Denny Sulijovic, and conducted between October 2022 and February 2023.

Acknowledgement

I am deeply grateful to the numerous individuals who have contributed their time, knowledge, and positive energy to support me throughout my master's thesis.

Above all, I extend my heartfelt thanks to Professor Anette Müllertz, my supervisor, for providing me with the opportunity to join the remarkable Physiological Pharmaceutics group. My experience working in the laboratory and in a research team has expanded my knowledge and skills immensely.

I also extend my sincere appreciation to my supervisor, Dr. Ondrej Holas, for his guidance and valuable input during my thesis. Additionally, I am grateful to my co-supervisor, PhD fellow Denny Suljovic, for being my best friend from day one and providing daily guidance. Thank you for your trust in my work and for the time we spent together in the laboratory.

I would like to express my gratitude to all the members of the Physiological Pharmaceutics group for their unwavering support and for organizing enjoyable social events. Special thanks to Lab Technician Yang Hwan Yun for being responsible and helpful in the laboratory and creating a safe working environment.

I extend my warmest appreciation to Professor Lucie Novakova and Ms. Hana Krieglerova for facilitating my participation in the Erasmus program and supporting me with my applications from the outset.

I thank my dear mother enough for being my greatest supporter and giving me the courage to pursue this degree. Without her, I would not have been able to reach this far and put in the effort required for this master's thesis.

Lastly, I want to thank my family and friends for their unwavering love and support. Special thanks to my sisters for always being there for me despite living in a different country ,for cheering me up and providing her endless support.

Abstract

Charles University, Faculty of Pharmacy in Hradec Králové Department of Pharmaceutical Technology
Supervisor: Dr. Ondrej Holas, Ph.D.
Consultant: prof. Anette Müllertz, Ph.D.
Student: Fatemeh Kheirabadi
Title of thesis: Study of the effect of biomolecules on the solubility of poorly soluble drugs

This thesis investigates the influence of proteins on the apparent solubility of drugs in fasted state stimulated colonic fluid. The investigation was conducted on a selection of compounds with varying physicochemical and plasma protein binding properties. Precisely, three different compounds named as Nilotinib, Carvedilol and Ritonavir were analyzed for their apparent solubility in three distinct protein sources: bovine serum albumin, mucin from dehydrated porcine gastric mucin type II, and collected porcine intestinal mucus.

Accurate reversed-phase high-performance liquid chromatography was developed and employed as the analytical method to determine the concentration of the apparent drug solubility of the investigated compounds.

The research on the solubility of poorly soluble compounds in simulated colonic fluid has been restricted. Additionally, factors such as the impact of proteins remains unexplored in biorelevant media, which could be critical for enhancing our understanding of drug solubility and protein binding in the colon.

The results of the study demonstrate that the presence of proteins in colonic fluid can significantly influence drug solubility. Specifically, the presence and increased concentration of proteins can enhance the apparent solubility of certain drugs with low water solubility.

These discoveries hold significant implications for pharmaceutical development, emphasizing the need to consider the influence of proteins in the colonic environment during the design of new drugs. The thesis contributes valuable insights into the intricate relationship between proteins and drug solubility in the colon.

The study also highlights the need for further research in this area, in order to better understand the mechanisms by which proteins affect drug solubility in the colonic environment.

Table of contents

List of Abbreviations

ABC transporter	ATP-binding cassette transporter
ACN	Acetonitrile
ADME	Absorption, distribution, metabolism, and elimination
AI	Artificial Intelligence
API	Active pharmaceutical ingredient
ATP	Adenosine triphosphate
BCR-ABL	Breakpoint Cluster Region - Abelson tyrosine kinase
BCRP	Breast Cancer Resistance Protein
BCS	Biopharmaceutics classification system
BSA	Bovine serum albumin
C18	Octadecyl
C8	Octyl
$CaCl_2$	Calcium dichloride
CAD	Charged aerosol detection
CDDS	Colonic drug delivery systems
CMC	Critical micelle concentration
DCM	Dichloromethane
DMSO	Dimethylsulfoxide
FaSSCoF	Fasted State Simulated colonic fluid
FaSSGF	Fasted State Simulated Gastric Fluid
FaSSIF	Fasted State Simulated Intestinal Fluid
GalNAc	N-Acetylgalactosamine
GI tract	Gastrointestinal tract
GRDDS	Gastroretentive drug delivery systems
HCF	Human colonic fluid
HCl	Hydrochloric acid
HFrEF	Heart Failure with Reduced Ejection Fraction
HPLC	High-performance liquid chromatography
IBD	Inflammatory bowel disease
IgA	Immunoglobulin A
KH_2PO_4	Potassium phosphate monobasic
Leu	Leucine
LOD	Limit of detection
LogP	Octan-water partition coefficient
LOQ	Limit of quantification
MCT1	Monocarboxylate Transporter 1
MDa	MegaDalton

MeOH	Methanol
$MgSO_4$	Magnesium sulfate
MQ Water	Milli-Q water
MRP3	Multidrug Resistance-Associated Protein 3
MRP4	Multidrug Resistance-Associated Protein 4
MUC-2	Mucin type II
Mw	Molecular weight
Na_3PO_4	Sodium phosphate
NaCl	Sodium chloride
NaOH	Sodium hydroxide
PBPK	Physiologically based pharmacokinetic modelling
PEG	Polyethylene glycol
PEPT1	Peptide transporter 1
P-gp	P-glycoprotein
Ph.Eur.	The European Pharmacopoeia
Phe	Phenylalanine
Phospholipids	PhosphatidyIcholine from soybean
PIM	Porcine intestinal mucus
Pro	Proline
PVP	Polyvinylpyrrolidone
RNA	Ribonucleic acid
RP-HPLC	Reversed-phase high-performance liquid chromatography
RP-HPLC-CAD	Reversed-phase high-performance liquid chromatography charged aerosol detection
RP-HPLC-UV	Reversed-phase high-performance liquid chromatography ultraviolet detection
RPM	Rounds per minute
R_t	Retention time
STP	Serine, threonine, and proline
TEN	Toxic epidermal necrolysis
TFA	Trifluoroacetic acid
Thr	Threonine
TRIS	Tris(hydroxymethyl)aminomethane
UV	Ultraviolet

1. Introduction

There has been limited research on the solubility and protein binding of compounds with poor aqueous solubility properties in colonic conditions. The efforts to improve the prediction of intra colonic solubility started in the early 2000s and the development of media that simulate colonic fluid was first achieved in 2010 by Vertzoni et al. However, there has been minimal further research in investigating the improvement of predicting intracolonic solubility and determining the apparent drug solubility in these media.[1]

Delivery systems for drugs that target the colon, known as colon-specific drug delivery systems (CDDS), are highly desirable for treating a variety of local diseases, including ulcerative colitis, Crohn's disease, irritable bowel syndrome, chronic pancreatitis, and colonic cancer.[2]

Furthermore, the colon can also be a potential site for systemic drug absorption for the treatment of non-colonic conditions. For example, drugs such as proteins and peptides which typically degrade in the extreme gastric pH environment can potentially be absorbed through the colon if delivered there intact.

For Orally administered drugs in colonic drug delivery, require the API to pass through the GI tract to achieve both local and systemic effect. Oral administration is the most common approach to drug delivery due to its safety, convenience, low cost, a greater degree of flexibility and better patient compliance. It is also a preferred route to drug administration for the treatment of chronic diseases that demand long-term drug administration [3,4].

Good absorption and high bioavailability are very important for the therapeutic efficacy of oral drugs. The efficiency of this process is subject to drug's physiochemical properties, like drug solubility [5,6], individual physiological characteristics, gastrointestinal pH, gastrointestinal transit time [7,8] and other factors like diet. Despite the promising outcomes of colonic drug delivery systems (CDDS) for drug absorption, due to longer transit time in the colon compared to the small intestine, their stability can be negatively affected by non-specific interactions with colonic content such as dietary residues, intestinal secretions, mucus, or fecal matter, as well as degradation by colonic bacterial enzymes, which can render the drug ineffective. Maintaining drug stability in the colon is therefore a concern. Another important factor is drug solubility, which can be limited by the low colonic luminal fluid volume, higher viscosity, and neutral pH, thus potentially becoming a rate-limiting factor for colonic absorption[9].

Simulated gastrointestinal media are commonly utilized in pharmaceutical research and development to predict the solubility and dissolution behavior of drugs and formulations. Several studies have shown that these media provide advantages over compendial media in predicting drug behavior in vivo [10,11].

Comparing results for different drugs is crucial for making informed decisions about the composition and production of new drug candidates. It is also essential to ensure that results from different laboratories around the world are comparable and can be confidently integrated into the development process, particularly in today's global working environment. Biorelevant media, also known as simulated gastrointestinal media, were first introduced in 1998 by Dressman et al [12]. These media aim to mimic the composition of gastrointestinal contents, including bile salts, fatty acids, and lipids, as well as to match the pH level, buffer capacity, osmolarity, and other factors. Biorelevant media are classified based on a classification system that determines their level of biorelevance and complexity, and they are available in both fed and fasted states [13].

While FaSSCoF (fasted state simulated colonic fluid) is considered as a useful tool for predicting oral drug absorption in the colon, it is important to note that the commercially available FaSSCoF media does not completely mimic the complex environment of the colon. The absence of naturally occurring proteins, enzymes, viscosity, and microorganisms in the media can impact drug absorption and metabolism, and thus the results should be interpreted with caution. Further research is needed to develop more biorelevant colonic media that can better simulate the complex environment of the colon. According to a study by Vertzoni et al. (2010), the average protein concentration of human colonic fluid in healthy fasted volunteers was found to be 9-12 mg/ml. It is important to note that the protein concentration may vary depending on various factors such as diet, health status, and age [1,13].

The presence of proteins in the colon can affect drug solubility and bioavailability, and therefore, further investigation of simulated colonic fluid and the impact of proteins present in the colon on drug solubility is important for better understanding and predicting the behavior of drugs delivered to the colon. it is essential to study the effect of proteins on drug solubility in simulated colonic fluid. This can be done by conducting experiments to determine the apparent drug solubility and protein binding properties of drugs in simulated colonic fluid, which can help in designing and optimizing colonic drug delivery systems.

1.1 Gastrointestinal Tract

The gastrointestinal (GI) system is responsible for numerous functions, including digestion, absorption, and excretion of ingested food and liquids, as well as providing protection against harmful microorganisms. The human GI tract is comprised of different organs and can be divided into two main parts: the upper and lower GI tract. The upper GI tract includes the mouth, esophagus, stomach, duodenum, jejunum, and ileum. The lower GI tract consists of the colon, rectum, and anus. Food is propelled through the esophagus into the stomach via coordinated esophageal peristalsis. In the stomach, the food bolus is mixed with gastric acid and digestive enzymes to form chyme, which passes through the pyloric sphincter into the duodenum. In the small intestine (duodenum, jejunum, and ileum), proteins, fats, and carbohydrates are broken down into smaller components for nutrient absorption. Once the luminal contents reach the large intestine, they are called feces and pass through the ascending colon, transverse colon and descending colon before being expelled via the rectum and anal canal [14].

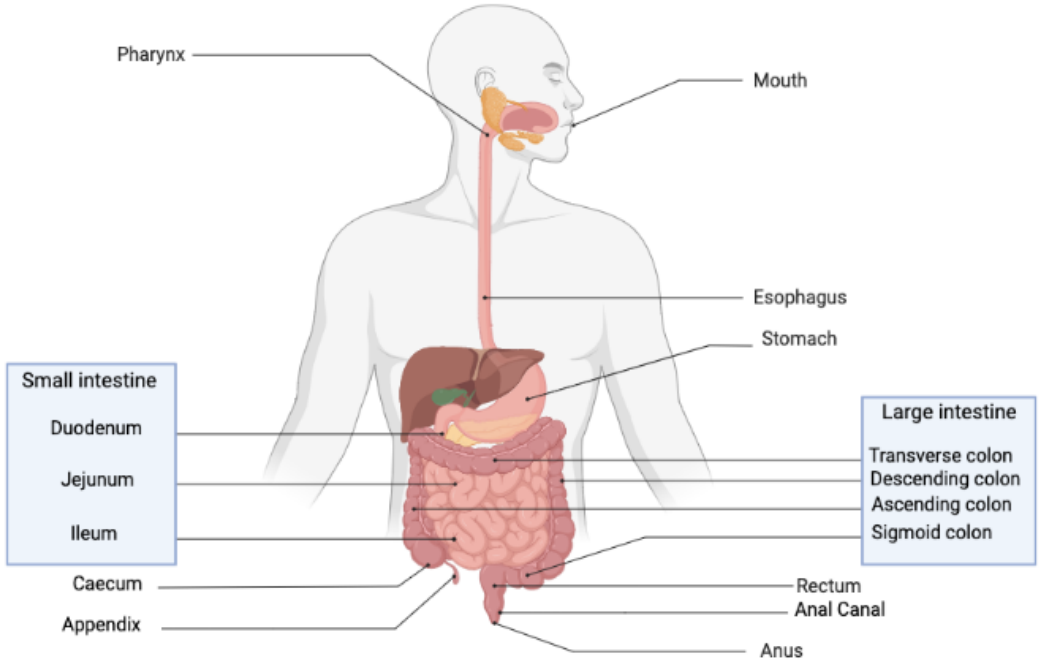

Figure 1: Human gastrointestinal tract anatomy. Created by BioRender.com

The gastrointestinal (GI) tract produces a substantial amount of fluid each day, up to 9 liters, which consists of digestive enzymes, bile, mucus, water, and ions. The process of nutrient breakdown begins with enzymatic reactions starting from the mouth and continues throughout the GI tract. Epithelial cells play a crucial role in the secretion and absorption of fluids, electrolytes, and solutes, and their structure and function vary depending on their location in the GI tract.

The stomach is an organ that contains glands responsible for secretion of gastric acid and intrinsic factor by gastric parietal cells within the gastric body. Chief cells within the gastric body secrete pepsinogen, while hormones such as gastrin, histamine, serotonin, and somatostatin are released from EEC throughout the stomach. Digestion and absorption of food and electrolytes occur mostly in the duodenum, jejunum, and ileum, where proteins, fats, and carbohydrates are broken down into smaller units by digestive enzymes such as amylase, lipase, and protease. These enzymes are primarily secreted from the pancreas [14] .

The transit time in different regions of the GI tract varies significantly. The passage from the mouth through the esophagus to the stomach is relatively quick, while the chyme remains in the stomach for approximately 2.5 to 4 hours. Once the acidic chyme enters the duodenum, the secretion of pancreatic juice and bicarbonate is stimulated by the hormones secretin and cholecystokinin, which also causes the gallbladder to contract and release bile. Bile salts play a role not only in aiding the digestion of lipids, they have also been found to enhance the absorption of other low water-soluble compounds.

Bile acids are amphipathic molecules and exist as bile salts in ionized form at the physiological pH in the intestine. The majority of bile salts exist in ionized form. In vertebrates, these bile salts are derived from cholesterol [29] , and thus their structures have the steroid nucleus, which comprises three six-carbon rings and one five-carbon ring. The common bile acids differ mainly in the number, position, and stereochemistry of hydroxyl groups in the steroid nucleus [30].

The small intestine is where the absorption of nutrients, particularly carbohydrates, proteins, and lipids, occurs. The transit time in the small intestine is typically around 3-5 hours. Finally, the nutrients are excreted as they travel from the colon to the rectum and are ultimately eliminated through the anus [15,27,30-34].

It was found that the pH in the human gastrointestinal (GI) tract varies significantly from the mouth to the anus according to a study conducted in 1999, that measured pH in the GI tract using two methods, intubation and pH-sensitive radio transmitting capsules. Saliva in the mouth has a pH range of 6.2-7.6, whereas the stomach has a highly acidic environment with a pH range of 1.0-2.0. The pH in the small intestine increases to approximately 6.0 in the duodenum and reaches about 7.4 in the terminal ileum. In the large intestine, the pH decreases to 5.7 in the caecum and then increases to 6.6 in the ascending colon and 7.0 in the descending colon [15].

The pH levels in the GI tract can be influenced by a variety of factors including age, sex, genetics, and whether if an individual is in a fed or fasted state. studies have shown that the pH in the stomach is generally lower in older adults than in younger adults, and that the pH in the colon is higher in women than in men. Additionally, certain medical conditions, medication use and life style habits such as smoking can also affect the pH levels in the GI tract.

the pH levels in the colon can also be affected by the types of microorganisms present in the gut microbiome, which can vary from person to person. The gut microbiota is the collection of bacteria, archaea an eukaryote residing the gastrointestinal (GI) tract [16]. It has been currently estimated that the number of the total microorganisms colonizing the GI tract is more than 100 trillion [17].

The density and diversity of the gut microbiota increases progressively from the small intestine to the large intestine (colon)[18]. Only fast-growing, facultative anaerobes which can adhere to epithelia or mucus are supposed to reside in the small intestine due to the limitations like a short transit time, lower pH, higher antimicrobial concentration and low levels of oxygen. The ileum and colon are the sites where the most plentiful gut microbiota exists [19,20].The predominant families of the gut microbiota in the colon are Bacteroidaceae, Prevotellaceae, Rikenellaceae, Lachnospiraceae and Ruminococcaceae [21]. The gut microbiota can provide numerous benefits to the host. In addition to its ability to extract energy, produce vitamins, and regulate bile acid metabolism, it can also offer protection against pathogens, regulate the host's immune system, and help maintain the integrity of the intestinal barrier [1,13,22]. Other factors that can also affect the composition of the gut microbiota include lifestyle, medications, stress, and certain diseases or medical conditions. For example, a high-fat or high-sugar diet can lead to changes in the gut microbiota composition, as can the use of proton pump inhibitors (PPIs) or non-steroidal anti-inflammatory drugs (NSAIDs). On the other hand, consuming fiber-rich foods and probiotics may promote a more diverse and healthier gut microbiota. Additionally, these microorganisms possess enzymatic activity that can directly or indirectly impact drug metabolism, such as the drug's biotransformation, first-pass effect, and enterohepatic recirculation as it is illustrated in figure 2. Additionally, the gut microbiota can affect the absorption of prodrugs and modify the metabolism of bile acids, thereby influencing the bioavailability of lipophilic drugs. Understanding the intricate relationship between the gut microbiota and oral drug absorption is crucial for comprehending inter-individual variations, providing personalized clinical advice, avoiding potential drug interactions, and designing innovative drug delivery systems, especially for colon-targeted delivery[23-28].

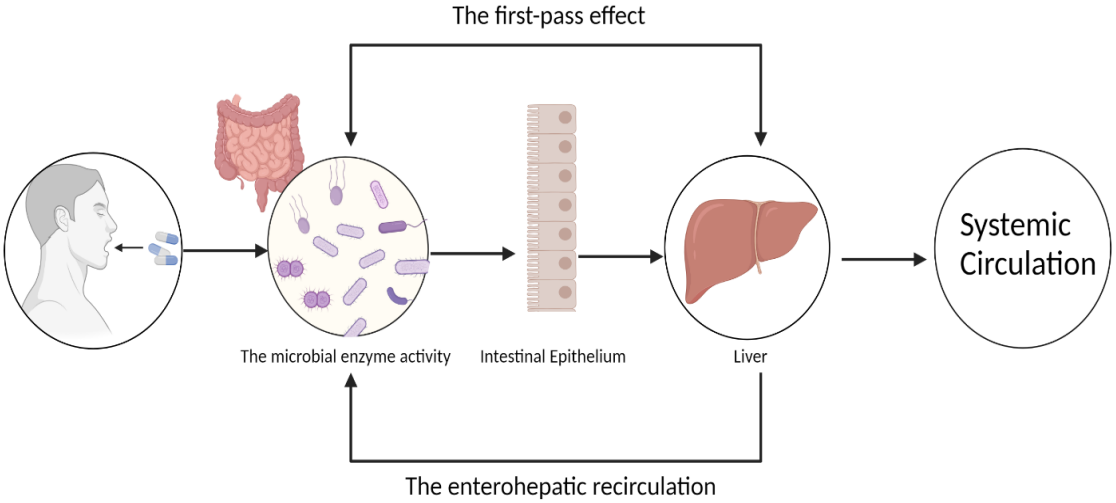

Figure 2: The figure illustrates the effects of gut microbial enzyme activity on the first-pass effect and enterohepatic recirculation of orally administered drugs. After oral administration, certain drugs undergo metabolism by microbial enzymes prior to absorption. Subsequently, these drugs and their metabolites are transported to the liver via the portal vein. Within the liver, hepatic enzymes facilitate processes such as oxidation and conjugation of the drugs. From there, the drugs and/or their metabolites can enter the systemic circulation or be redirected back to the intestine, where they can be reactivated by microbial enzymes or other gut enzymes before being transported once again to the liver. It is important to note that both the first-pass effect and enterohepatic recirculation significantly influence the bioavailability of oral drugs. Created by BioRender.com [28]

1.2 Small Intestine

The small intestine plays an important role in digestion, secretion, and absorption of nutrients. Although the functional surface area of the small intestine is only one cell thick, it is greatly increased by the presence of numerous mucosal folds that contain finger-like projections called villi. Each villus is made up of 2000-8000 epithelial cells and is surrounded by 6-14 crypts of Lieberkühn. the intestinal surface involved in digestion and absorption is significantly increased by the presence of villi and microvilli on the enterocytes. The height of the villi and the depth of the crypt decrease from the proximal towards distal part of the gut, while the number of goblet cells (which produce mucus) increases[35].

While mucus found throughout the gastrointestinal tract contains the same biological components, the properties of the mucus differ depending on its regional function. In the small intestine, the mucus is only one layer thick and is loosely attached to the epithelium, allowing for efficient nutrient absorption by the host epithelium. This single layer mucus is easily penetrable, which is important for the absorptive function of this region as well as for release of digestive enzymes located in the brush border membrane of the epithelial cells.

The small intestine's mucosal barrier contains antibacterial mediators like defensins, lysozymes, and other peptides that are released by Paneth cells to regulate the bacterial content in the region (Peterson et al., 2007). This defense mechanism is crucial as the mucus layer in the small intestine is loosely attached and easily penetrable, making it easier for foreign particles to invade. To counter this, the small intestine has a higher density of Paneth cells and corresponding peptides, which help maintain epithelial crypts and neutralize foreign invasions (Ouellette, 2010) [36].

1.3 Colon

The colon, which is around 165 cm in length in humans, receives approximately 400-500 ml of alkaline chyme daily. Its main function is to absorb water, electrolytes, short-chain fatty acids, and bacterial metabolites in healthy adults.

The colon has an internal lining that is made up of simple columnar epithelium but lacks villi, which results in a relatively small absorptive area and slow absorption compared to the small intestine. The colon also has other distinguishing landmarks, such as the ileocecal valve, a muscular valve that separates the small bowel and cecum, and the appendix [37,38].

The large intestinal epithelium has tighter cell junctions compared to the small intestine, which prevents ions from back-diffusing through these junctions. As a result, sodium ion absorption is more complete in the large intestine compared to the small intestine [35].The colon also has a different absorption process for some substances, such as glucose, galactose, and tyrosine, which are absorbed by active transport in the small intestine but not in the colon [39]. The colonic epithelium lacks a continuous layer of longitudinal smooth muscle, which renders it incapable of peristaltic contractions. This structural difference results in a longer transit time of contents through the colon [35]. in healthy adults, colonic transit normally requires several hours to almost 3 days for completion.

While the colon is generally considered a single organ, there are differences in both structure and function between the right and left sides. The right and left colon have independent activity, with the right side typically exhibiting more activity than the left, including non-propulsive contractions [37].

Furthermore, the colon differs from the small intestine in terms of enzyme expression. Unlike the small intestine, the colon does not express any digestive enzymes. However, the colon does contain enzymes such as cytochrome P450 isozymes and uridine diphosphate (UDP)-glucuronosyltransferase, which are involved in drug metabolism. These enzymes are important considerations in the development of colonic drug delivery systems [35].

The colon is home to a large number of both aerobic and anaerobic bacteria. It is estimated that there are 10^{13}–10^{14} commensal bacteria in the adult intestine, which is more than the number of cells in the human body. The intestine provides nutrients that can be utilized by these bacteria and the temperature is also optimal for their growth. These bacteria possess biotransformation enzymes, such as beta-glucuronidases, beta2-glycosidases, demethylases, hydrolases, and reductases, which are capable of metabolizing drugs and biomolecules. The diversity of these microbiota and their enzymes can have an impact on drug delivery systems targeted to the colon [33,40].

The colon's bacterial ecosystem is vital for maintaining homeostasis and assisting in the digestion of carbohydrates that are not digested in the upper gastrointestinal tract. These bacteria are well-tolerated by the human immune system and do not trigger an inflammatory response under normal conditions due to the outer mucosal layer of colonic epithelia [35,41]

1.3.1 Colonic Mucus

The mucus layer serves as the first line of defense against microorganisms, digestive enzymes, acids, digested food particles, microbial by-products, and food-associated toxins that may invade the gastrointestinal (GI) tract. This layer lubricates the contents of the lumen and acts as a physical barrier against bacteria and other antigenic substances. The moist, nutrient-rich mucus layer next to the epithelial barrier of the GI tract is essential for maintaining intestinal homeostasis and contains a thriving biofilm of both beneficial and pathogenic microbial populations [36]. Various factors can influence the volume of the mucus layer. Substances such as pilocarpine, histamine, acetylcholine, or stimulation of the parasympathetic nerves, as well as aspirin, NSAIDs, bile acids, cigarette smoke, and inflammation, can increase the volume. Conversely, atropine, barbiturates, or stimulation of the sympathetic nerves can decrease its volume [35].

The composition of mucus is mainly water, making up about 98% of its content. However, it also contains other components such as bicarbonate, proteins, carbohydrates, phospholipids, salts, IgA, and cholesterol [42,43]. Mucus is primarily formed by the branched glycoprotein mucin, which is secreted from goblet cells located in the epithelial lining of the gastrointestinal tract. Goblet cells are found in both the villi and crypts of the small intestine and the colon [44] It is important to note that the organization of the mucus layer is not uniform throughout the GI tract. In the stomach and colon, there are two distinct mucus layers are present. The inner layer is firmly attached to the mucus-producing goblet cells of the epithelial membrane, while the outer layer is loosely adherent and provides a habitat for bacteria. In contrast, in the small

intestine, the mucus layer is secreted at the top of the crypts and then transported upwards between the villi in a discontinuous layer. Therefore, this layer is not always covered with mucus. As explained in figure 3 [41] . Although the thickness of the human gastrointestinal mucus has not been precisely measured, it is known that the colon has the thickest mucus layer compared to the small intestine and stomach. The outer mucus layer is estimated to be twice as thick as the inner layer and varies greatly in thickness, depending on the level of bacterial flora present. This outer layer is degraded by bacterial flora, and thus only foreign bacteria can be found within it [41]. The mucus layer in the colon can pose a challenge for drug delivery systems as it acts as a barrier that must be penetrated for drugs to be absorbed into the bloodstream. The properties of the colonic mucus layer, such as pH and water content, can also affect drug absorption. Additionally, the physicochemical interactions between the drug and

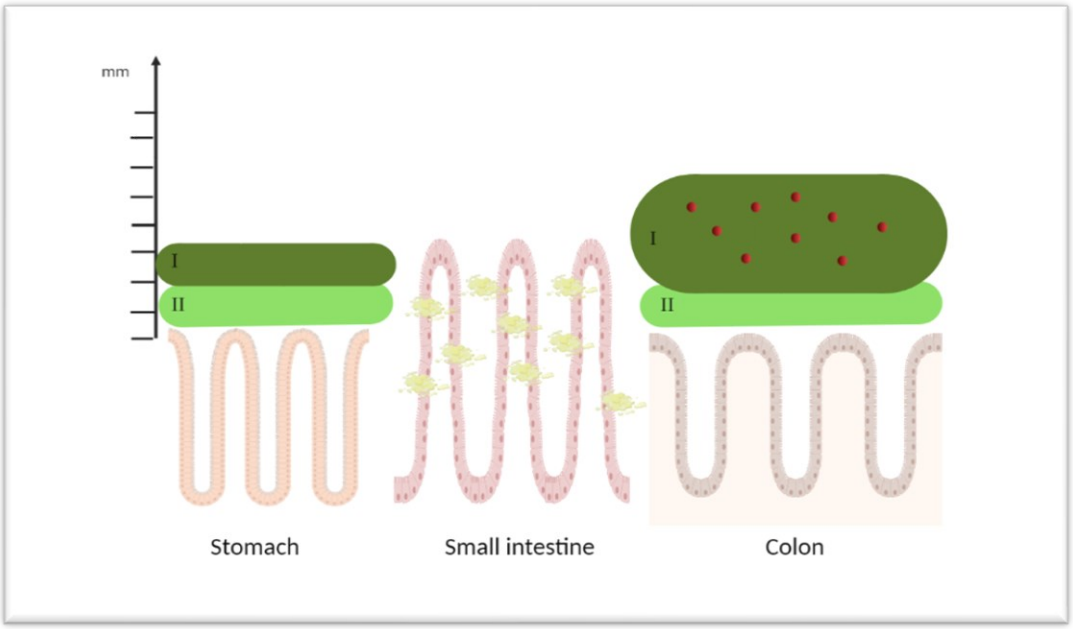

Figure 3: A schematic illustration of the mucus thickness on the epithelium in the GI tract. The thickness expressed in mm. The dark green color expresses the outer mucus layer, named I. The lighter green color expresses the inner mucus layer, named II. the red dots express the foreign bacterial microorganism [41]. Created with BioRender.com

protein sources, such as the glycoprotein mucin, may affect the drug's diffusion and solubility [45].

1.3.2 Proteins Found in the Colon

Proteins present in the colon come from different sources, with the primary source being the glycoprotein mucin, particularly MUC2 mucin. There are over 20 different subtypes of mucin found in human, which are distributed differently throughout the gastrointestinal (GI) tract. For instance, the salivary glands produce MUC5B and MUC7 to lubricate food, while the stomach's mucus layer contains MUC5AC, and the main component of mucus in the small intestine and

colon is Mucin-2. These differences in mucin subtypes reflect the specific functions and needs of each section of the GI tract [36].

Mucin is composed of monomers with a molecular mass of about 2.5 MDa, where the protein core accounts for 20% of the mass, and the rest consists of glycans. These monomers are linked covalently as dimers at the C-terminus and trimers at the N-terminus, creating large net-like structures. Prior to release into the intestinal lumen, MUC2 is stored in goblet cell granules assembled on a calcium-dependent ring-shaped platform formed by MUC2 N-termini interactions. When released, the mucin unfolds and expands over 1,000-fold in volume, likely due to the chelation of calcium by bicarbonate. The formed nets spontaneously organize into flat sheets that stack on top of each other to form the lamellar inner mucus layer, which remains anchored to the epithelial cells and acts as a barrier that does not allow bacteria to penetrate [44].

Mucins are large glycoproteins consisting of over 80% carbohydrates that concentrate into mucin domains. These domains are built on a protein core rich in the amino acids, proline, serine, and threonine, forming STP-repeats with carboxy and amino terminals, giving the mucin molecule both hydrophilic and hydrophobic interactions. The STP-repeats sequences can be quite long, with the largest one in MUC2 being about 2,300 amino acids. N Acetylgalactosamine (GalNAc) which is an amino sugar derivative of galactose is added to the hydroxyl group of the amino acids serine and threonine by alpha-1-O-glycosidic bonds, which extends the mucin domains into long rods, covered with glycans so densely that the protein core is completely protected from protease degradation. The mucin domain glycans bind a lot of water and generate most of the gel-like properties of mucins. The primary role of gel-forming mucins is to create mucus that safeguards and lubricates the gastrointestinal tract in conjunction with other components. According to Caldara et al.38, mucus that is freshly produced is not adhesive or hydrophobic, and these characteristics only develop when mucus is stored or purified [42], [44]. The bulk of proteins present in mucus are mucin glycoproteins, but it has been observed and mentioned in other studies that serum proteins such as albumin can also be detected in mucus. These serum proteins are believed to originate from epithelial serum transudation [42]. The most abundant Serum protein which is derived from plasma serum is albumin. Albumin functions as a carrier for various substances such as drugs, peptides, and fatty acids in the blood plasma due to its high binding affinity. Unlike mucin, albumin is a non-glycosylated protein and exists in a monomeric form [46]. Additionally, proteins from food intake can also be detected in the colonic fluid [22].

1.3.3 Colonic Transporters

The movement of drugs across the intestinal wall is a complex process that involves various factors, including drug metabolizing enzymes and protein transporters. Drug transporters, in particular, are critical components of the functional barrier of the intestine. These transmembrane proteins are found on the apical and basolateral membranes of enterocytes and are responsible for the cellular uptake or efflux of endogenous compounds, nutrients, and xenobiotic compounds. They play a key role in determining drug absorption by regulating the movement of drugs into and out of cells. In this regard, the expression and activity of uptake and efflux transporters can significantly influence drug absorption in the colon.

Functionally, transporters can be classified into two principal classes, ABC (ATP-binding cassette transporter) transporters that mediate extracellular efflux, and SLC carriers that mediate cellular influx and/or cellular efflux. P-gp (P-glycoprotein) and BCRP (Breast Cancer Resistance Protein) are efflux transporters, while PEPT1 (Peptide transporter 1) is an uptake transporter. These transporters show increased expression from the duodenum to distal jejunum and ileum, and their expression significantly drops in the colon. CYP3A5, CYP2B6, CYP2J2, CYP3A4, and CYP2C9 are some of the metabolizing enzymes found in the duodenum and jejunum, but their expression decreases significantly in the ileum and colon [47].Overall, the expression of drug uptake and efflux transporters, as well as cytochrome P450 (CYP450) enzymes on the epithelium of the colon is lower compared to the small intestine [45].

This characteristic provides several opportunities for colonic drug delivery. This is especially beneficial for drugs that are significantly effluxed by apical membrane transporters or inactivated by CYP450s in the small intestine, as they can achieve increased bioavailability when released in the colon. For instance, simvastatin demonstrates three times higher bioavailability when formulated for delayed rather than immediate gastrointestinal release, as it avoids small intestinal CYP450s However, some transporters such as MRP3 (Multidrug Resistance-Associated Protein 3), MCT1 (Monocarboxylate Transporter 1), and exhibit increased expression in the colon compared to the small intestine. Additionally, the presence of diseases such as inflammatory bowel disease (IBD), particularly during acute inflammation, can alter transporter expression in the colon. This alteration can result in lower expression of P-gp, MRP4 (Multidrug Resistance-Associated Protein 4) , MCT1, and BCRP on colonocytes in IBD patients compared to healthy individuals, while MRP2 expression may increase [48]. While transporters play a critical role in determining drug absorption in the intestine, their expression levels vary significantly throughout the tract. This has important implications for drug development and formulation, as colonic drug delivery may provide increased bioavailability for some drugs. However, the impact of disease states like IBD on transporter expression underscores the need for further research in this area.

1.4 Solubility

Solubility is a crucial characteristic when it comes to drug delivery and bioavailability. It refers to the ability of a drug substance to dissolve in different solvents. Essentially, solubility can be defined as the amount of a substance that can dissolve in a given amount of another substance. This is typically measured by determining the number of milliliter of solvents required to dissolve 1 gram of solute at a particular temperature and pressure. Pharmacopoeias define solubility in specific solvents, such as water and certain organic solvents. The European Pharmacopoeia (Ph.Eur.) outlines different levels of solubility in grams of solvent per gram of solute, as shown in the accompanying table.

Table 1: Ph.Eur.definition of terms in solubility is referred to temperature between 15°C and 25°C.[49]

Descriptive term	Solubility (g/ml)
Very soluble	<1 part solvent needed to dissolve 1-part solute
Freely soluble	1-10 parts solvent needed to dissolve 1-part solute
Soluble	10-30 parts solvent needed to dissolve 1-part solute
Sparingly soluble	30-100 parts solvent needed to dissolve 1-part solute
Slightly soluble	100-1000parts solvent needed to dissolve 1 part solute
Very slightly soluble	1000-10000parts solvent needed to dissolve 1-part solute
Practically insoluble	>10000 parts solvent needed to dissolve 1-part solute

Solubility is a complex phenomenon that occurs when a solid active pharmaceutical ingredient (API) dissolves in a solvent or mixed solvent. This process involves a dynamic equilibrium between the forces of dissolution and reprecipitation. Several methods can be used to define solubility for an API, such as kinetic, thermodynamic, intrinsic, and apparent solubility.
In practical applications, thermodynamic solubility is often referred to as equilibrium solubility, which is the concentration limit reached at thermodynamic equilibrium or saturated solubility, where a saturated solution is utilized to confirm that the concentration limit has been achieved. Apparent solubility is another type of solubility that sometimes known as 'true solubility' is the concentration experimentally measured of a solute in a solvent out of equilibrium conditions.
For this particular thesis, the focus will be on the concept of apparent solubility. Apparent solubility can be higher than equilibrium solubility if supersaturation is generated by the drug delivery system, or it can be lower than equilibrium solubility if the time required to reach equilibrium is insufficient. Intrinsic solubility, on the other hand, is the concentration of the neutral solute in a specific pH range where the neutral molecules are dominant [50,51].

1.4.1 Factors Affecting Solubility

The solubility of a solid-state form of a solute in a particular solvent is determined by the interactions between the drug molecules in the solid-state form and the intermolecular interactions between the drug and solvent molecules in solution. These interactions involve both enthalpic and entropic terms, and as a result, the solubility of solutes in solvents is temperature-dependent and generally increases with temperature. The standard temperature for determining solubility is 25°C, unless otherwise specified. The pressure's effect on drug solubility is generally of limited significance in the in vivo situation, although it may play a role during manufacturing.

The pH of the solution also plays a critical role in the solubility of an active pharmaceutical ingredient (API) that undergoes ionization from a non-ionized to an ionized form. Since many drugs are weak acids or bases, the solubility of such compounds is highly dependent on the solution's pH and ionization constants (Ka). Therefore, adjusting the pH to manipulate the solubility is the most common approach to increasing the solubility of low-solubility drugs.

The solubility of a compound with a basic anion increases as the acidity of the solution (pH) decreases, due to Le Châtelier's principle. For weak acids, this relationship can be approximated by the solubility at pH values more than one unit below the pKa. At higher pH values, the solubility of the acid increases because of the contribution from the ionized form. The relationship between the logarithm of the solubility and pH is linear until the limiting solubility of the ionized form is reached. The opposite is true for weak bases.

The saturation solubility of ionizable drugs is strongly influenced by the pH of gastrointestinal fluids, which can vary widely between different parts of the gastrointestinal tract. Factors such as age, pathophysiological conditions, and concurrent drug therapy can also affect the pH of the luminal fluids. For poorly soluble weak bases like ketoconazole and itraconazole, elevated gastric pH in AIDS patients can lead to reduced drug dissolution and malabsorption. In contrast, fluconazole has a high enough solubility that elevated gastric pH does not limit its absorption. Other physiochemical properties such as molecular weight and polymorphism can also impact solubility [50,52,53].

1.4.2 Apparent Solubility in Biorelevant Media

The gastrointestinal (GI) tract is a complex system with various compartments, significant variations in pH and ionic strength, and the presence of natural surfactants like bile acids. Consequently, even the methods used to determine pH-dependent solubility do not provide a complete understanding of the drug's solubility behavior in the GI tract, which is critical for absorption considerations. To address this, biorelevant media have been developed to more accurately estimate drug solubility in the gastric or duodenal environment, with or without digested food components, to provide better in vitro determination of drug solubility [50,52]. Vertzoni et al. (2005)[1] have reported a strong correlation between solubilities measured in biorelevant media and in human gastrointestinal fluids. In order to improve the matching of solubilities in human fluids, several versions of biorelevant media have been proposed, and their physical-chemical properties such as pH, surface tension, osmolality, and buffer capacity were adjusted (Dressman et al., 1998; Jantratid et al., 2008; Marques et al., 2011)[13,54,55]. Furthermore, biorelevant media were developed to simulate the fed and fasted state for different regions in the GI tract. Recently, Markopoulos et al. (2015) [55] proposed a decision tree to determine the appropriate level of complexity of biorelevant media based on the drug type, dosage forms, and dosing conditions. This decision presented four levels of simulation of luminal compositions.

Level 0 media are simple aqueous solutions where the pH is adjusted to mimic the pH of specific intestinal region. The compendial buffer solutions and SGF or SIF without enzymes described above could be used as level 0 media.

Level I media mimic both the pH and buffer capacity of specific intestinal region.

Level II media comprise in addition to above, bile components, dietary lipids, lipid digestion products and have an adjusted osmolality. These compositions better reflect the solubilization capacity of luminal fluids and the impact of fasted/fed dosing conditions. And is the highest level yet achieved in the development of biorelevant media.

Level III media contain dietary proteins and enzymes (in place of digestion products from Level II) to address the impact of digestion and viscosity on the drug release. In figure 4 the classification of the level of biorelevant media and complexicity are shown [51].

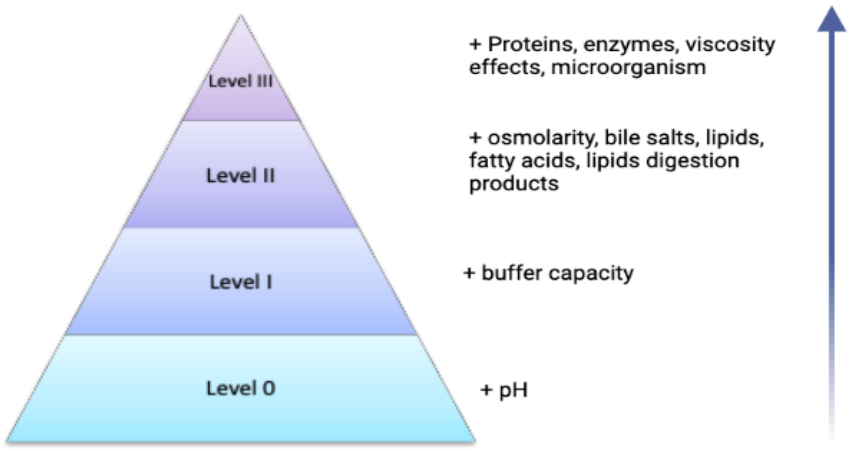

Figure 4: The classification of biorelevant media levels, with level 0 representing the lowest biorelevance and complexity, and level III having the highest. The figure also provides a visual representation of the additional components needed to achieve each level. Created with BioRender.com

Choosing the appropriate biorelevant media is crucial, particularly when testing drug products that contain poorly soluble drugs. It is important to select a medium that not only replicates the pH and buffer capacity of the gastrointestinal tract, but also includes bile components such as bile salts, phospholipids, and cholesterol [56].

In the small intestine, the presence of amphiphilic bile components, including bile salts, lecithin, and monooleins, can enhance drug solubility. Micellar solubilization of the drug can occur when these substances are present in concentrations higher than their critical micelle concentration (CMC).

Numerous studies have reported solubilization into simple bile salt micelles for a variety of poorly soluble drugs, such as griseofulvin, glutethimide, digoxin, leucotriene-D4 antagonists, and gemfibrozil. Addition of physiological concentrations of bile salts to aqueous media has been shown to increase solubility up to 100-fold [53].Ensuring the stability of biorelevant media is crucial when using them in experiments. Initially, it was necessary to prepare the media freshly from individual ingredients for each experiment. However, instant powder versions of several biorelevant media are now commercially available, making them as simple to prepare as compendial media. Experiments have demonstrated that fasted stimulated gastric fluid (FaSSGF) does not require an equilibrium time and can be stored at ambient temperature for up to 96 hours. Similarly, FaSSCoF can be stored for up to 48 hours and reaches equilibrium 2 hours after preparation [1,57].It should be noted that the buffer capacity of the fasted state medium is low, which can cause a pH change when using weak bases/ acids. Therefore, it is essential to check the pH of the sample solution and correct it if necessary[13].

1.4.3 Bioavailability and permeability evaluation

Investigating the physiochemical properties and absorption, distribution, metabolism and elimination (ADME) profile of a compound is essential during drug development. The bioavailability of orally administered compounds can be classified using the Biopharmaceutics Classification System (BCS), which takes into account the compound's aqueous solubility and intestinal permeability. The BCS has four classes based on the administered dose, as showed in figure below [58].

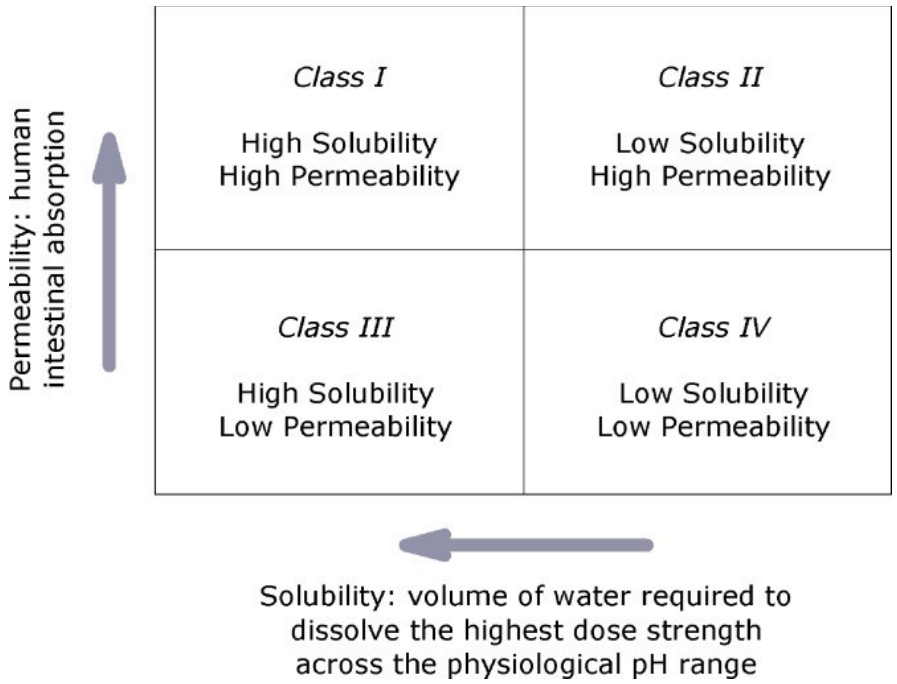

Figure 5: The biopharmaceutics classification system. [59]

This system considers the solubility, permeability, and dose of a drug, while the DCS approach includes dissolution rate and distinguishes between solubility-limited absorption and dissolution-limited absorption. The use of pharmacokinetic simulation software is also common to understand the behavior of a research compound in humans and animals, including dissolution, solubility, and precipitation in the GI tract [52].

Formulation strategies to address these issues fall into two categories: methods that increase drug solubility and dissolution rate, and techniques that increase dissolution rate and facilitate the formation of supersaturated drug solutions. Advanced techniques that combine both approaches are also available [51].

Lipinski's Rule of 5 is a useful tool for assessing the permeability of a compound. It consists of four criteria that a compound must meet to have a theoretically high permeability, which are

listed in the table below. It should be noted that the molecules investigated in this thesis are small molecules with varying physicochemical properties, including octanol-water partition coefficient (Log P) and pKa values. These properties will be discussed in detail in another chapter [60].

Table 2: Criteria for Lipinski's Rule.[60]

MW	≤ 500 g/mol
Log P	≤ 5
Hydrogen bond acceptor	≤ 10
Hydrogen bond donnor	≤ 5

1.4.4 Poorly Soluble Drugs

The ability of a drug to dissolve and enter a solution can sometimes be a more significant barrier to absorption than its ability to pass through the intestinal mucosa. Even for drugs that can easily cross the intestinal lining, the onset of the drug's effect may depend on the time it takes for the medication to release and dissolve in the body. A drug is considered "poorly soluble" when its dissolution rate is so slow that it takes longer than the time it takes to pass the absorptive sites, which leads to incomplete bioavailability.

The aqueous solubility of a drug plays a vital role in its dissolution rate, and "poorly soluble" drugs generally have an aqueous solubility of less than 100 mg/mL. Another factor used to identify "poorly soluble" drugs is the dose: solubility ratio, which refers to the volume of gastrointestinal fluids required to dissolve the administered dose. When this volume is more significant than the available fluids, incomplete bioavailability may result from solid oral dosage forms.

The dissolution rate of a drug can be explained through the modification of the Noyes-Whitney equation (Equation 1), which takes into account several factors, including surface area, diffusion coefficient, boundary layer thickness, saturation solubility, dissolved drug amount, and volume of dissolution media. Many physicochemical and physiological factors can influence the factors in the equation and the dissolution rate, including the crystalline form of the drug, its lipophilicity, its ability to be solubilized by native surfactants and co-ingested foodstuffs, its aqueous solubility, pKa, and the gastrointestinal pH profile [53].

$$\frac{dM}{dt} = \frac{D\,S}{h}(C_s - C)$$

Equation 1. Noyes-Whitney equation

The pharmaceutical development of poorly water-soluble drugs can be challenging due to their limited solubility, which can lead to lower bioavailability and therapeutic efficacy. To address this issue, there have been increasing efforts to improve the solubility of these drugs to enhance their pharmacokinetics and pharmacodynamics.

1.5 Tested Drugs

In the field of drug development, many newly discovered drugs candidates exhibit poor solubility and/or permeability. This leads to a low and inconsistent oral bioavailability when administered in oral dosage forms. Consequently, it becomes imperative to explore their solubility behavior in different parts of the gastrointestinal tract (GIT) and to develop bio enabling formulation technologies that can enhance their biopharmaceutical properties and improve their oral absorption. Several approaches have been extensively reviewed in this regard, including solid dispersions, lipid-based formulations, and nano-sized drug crystals/particles.

For the purpose of this study, we have selected three well-known drugs, namely Nilotinib, Carvedilol, and Ritonavir, which are commonly used in clinical practice and belong to diverse therapeutic classes, including anticancer, cardiovascular, and antiviral, respectively. These drugs have been chosen based on previous research that indicates their poor water solubility, which in turn, leads to low oral bioavailability. Therefore, these drugs are ideal candidates for investigating the impact of Colonic proteins on their solubility and for improving their solubility through formulation approaches. Additionally, these drugs belong to different BCS classes, with Carvedilol being a BCS Class II drug with low aqueous solubility and high permeability, and Ritonavir and Nilotinib being BCS Class IV drugs with high aqueous solubility and low permeability, respectively.

Furthermore, the selected drugs were chosen because of their distinct physicochemical properties, including molecular weight, pKa, degrees of lipophilicity, and different chemical structures. These differences may influence their protein binding and different solubility behavior in simulated colonic fluid. Additionally, these drugs have been previously utilized in clinical trials and have established pharmacokinetic and pharmacodynamic profiles, which makes them ideal candidates for this study.

1.5.1 Nilotinib

Nilotinib is a synthetic aminopyrimidine and a second-generation ATP-competitive inhibitor of BCR-ABL (Breakpoint Cluster Region - Abelson tyrosine kinase). It is highly selective for BCR-ABL and binds to wild-type BCR-ABL with 20-50 times more affinity than imatinib. Nilotinib is formulated as 200 mg hard capsules and is approved for oral administration to treat chronic phase and accelerated phase Philadelphia chromosome-positive chronic myelogenous leukemia (Ph+ CML) in patients who are resistant to or intolerant of at least one prior therapy, including imatinib. Nilotinib has a well-established efficacy and safety profile.Nilotinib is member of several chemical groups, including (trifluoromethyl)benzenes, pyrimidines, pyridines, imidazoles, secondary amino compounds, and secondary carboxamides. Its functions include being an antineoplastic agent, a tyrosine kinase inhibitor, and an anticoronaviral agent. The compound has a molecular mass of 529.5 $g \cdot mol^{-1}$ and is formulated as a hydrogen chloride monohydrate salt. It appears as a white to slightly yellowish or slightly greenish-yellowish powder.

Nilotinib is classified as a weak base, with a pKa1 value of 3.0 and pKa2 value of approximately 6.2. The active compound has no chiral center and, therefore, is not optically active as illustrated by its structure in Figure 6.[61] Numerous crystal hydrates and solvates of nilotinib hydrochloride monohydrate have been identified to date, including Forms A, B, C, and amorphous. Form A corresponds to a dihydrate form, while Form B and Form C are monohydrate forms obtained after desolvation of different solvates. Form B is the most stable form, isolated from the synthetic process and utilized in medicinal products, with the least hygroscopic behavior among Forms A, B, and C. Stability studies have showed no transformation in any of the three forms even after several months of storage at room temperature. However, it's worth noting that the active substance is slightly light-sensitive.

The solubility of nilotinib hydrochloride monohydrate in aqueous solutions is 2.4X10-3 mg/L at 25°C. [62]. This solubility decreases significantly as the pH increases, and it becomes almost insoluble in buffer solutions with pH values of 4.5 and above. Nilotinib has low solubility in ethanol and methanol and is almost insoluble (<0.1 mg/mL) in a phosphate buffer with pH >4.5. Nilotinib is a moderately permeable compound, with a Caco-2 permeability of $2.7 \times 10{-}6$ cm/s and an estimated human permeability of approximately $1.5 \times 10{-}4$ cm/s. Consequently, it is provisionally classified as a Class IV compound according to the Biopharmaceutics Classification System (BCS) due to its low/moderate aqueous solubility and moderate permeability [63]. Due to its poor aqueous solubility, no intravenous formulations of nilotinib have been developed for human investigation, and its absolute oral bioavailability could not be determined based on clinical data.

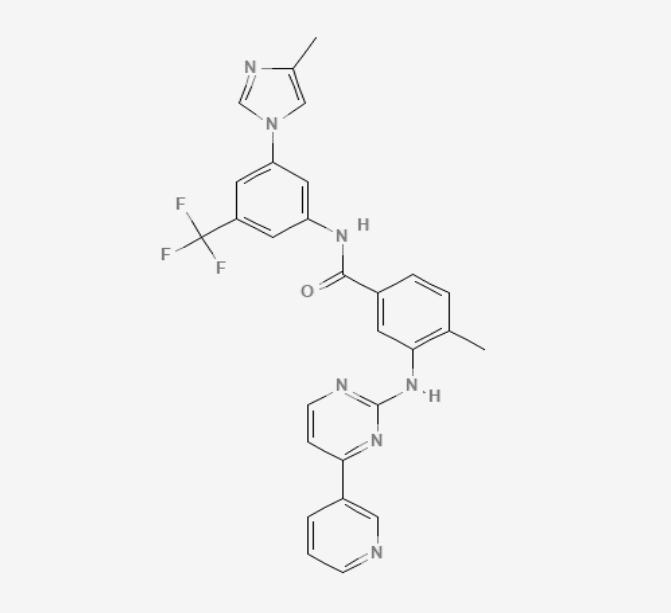

Figure 6: Chemical structure of Nilotinib, a compound also known as nilotinib hydrochloride monohydrate. Its chemical name is 4-methyl-N-[3-(4-methyl-1H-imidazol1-yI)-5-(trifluoromethyl)phenyl]-3-[(4-pyridin-3-ylpyrimidin-2-yl)amino] benzamide hydrochloride monohydrate, and its molecular formula is C28H22F3N7O·HCl·H2O. This compound lacks a chiral center and cannot undergo tautomerism. [62]

Nilotinib has primary pharmacodynamics effects on human Philadelphia-positive CML(chronic myelogenous leukemia) cells as well as transfected murine hematopoietic cells. It inhibits the auto-phosphorylation of native BCR-ABL in cell lines such as K-562, KU812F, 32D, and Ba/F3 with IC50 values ranging between 20 to 60 nM. On the other hand, cells that do not express BCR-ABL exhibit resistance to nilotinib below 2 μM. Nilotinib is also effective against various mutant forms of BCR-ABL that have shown resistance to imatinib. It has the ability to inhibit autophosphorylation and proliferation of 33 out of 34 BCR-ABL mutants with IC50 values ranging from 20 to 800 nM.

Various pharmacokinetic studies conducted in vitro and in vivo have revealed that the plasma protein binding of nilotinib is high, with an average of 97.4%, 99.1%, 98.2%, 99.0%, and 98.4% in mouse, rat, dog, monkey, and human, respectively. The blood-to-plasma concentration ratios of nilotinib were less than one in humans, at 0.68. An important property for our study is that nilotinib is highly bound to human serum albumin and α-1 acid glycoprotein, at 93.4 to 93.9%, and heparin has no effect on the protein binding of nilotinib in human plasma.

In vitro data indicate that the metabolism of nilotinib primarily occurs in the liver and involves various reactions, such as the oxidation of the methyl-imidazole ring, degradation of the oxidized imidazole, , amide hydrolysis, glucuronic acid conjugation with the parent compound or metabolites, and various combinations of these reactions, which are mediated by the cytochrome P450 (CYP) 3A4 enzyme.

In humans, unchanged nilotinib is the primary circulating component in human serum,

accounting for 88% of the AUC0-48h. The two highest metabolites present in human serum are P36.5 and P41.6, with AUC0-48h values of 6.9% and 5.3%, respectively, relative to the unchanged drug. These metabolites are formed through a common biotransformation pathway where the methyl group in the methylimidazolam moiety of nilotinib is hydroxylated initially (P41.6) and then further oxidized to a carboxylic acid (P36.5). Additional metabolic pathways observed in humans include hydroxylation of the methyl group in the amino-methyl-benzamide moiety (P42.1), N-oxide formation on the pyridine nitrogen (P36), oxidative/hydrolytic degradation of the midazolam ring leading to multiple products, oxygenation of the pyridinyl-pyrimidinyl-tolyl-amine and methyl-phenyl-imidazole moieties, and cleavage of the amide linkage (P20). P36 and P42.1 were found in human serum with AUC0-48h values of 0.58% and 1.5%, respectively, relative to the unchanged drug. The combination of these primary biotransformation pathways leads to the observation of twenty distinct human metabolites of nilotinib[62].

In vitro studies have also shown that nilotinib is a competitive inhibitor of CYP3A4/5, CYP2C8, CYP2C9, CYP2D6, and uridine diphosphate glucuronosyltransferase 1A1 (UGT1A1)[64]. Furthermore, nilotinib can be considered an in vitro inducer of CYP2B6, CYP2C8, and CYP2C9 activities.

Nilotinib is generally well-tolerated by most patients, but like all medications, it can cause side effects. The most common side effects of nilotinib include nausea, diarrhea, vomiting, fatigue, myalgia and joint pain, headache, skin rash, pruritus (itching), and fever. Less common side effects may include fluid retention, shortness of breath, thrombocytopenia (low blood platelet counts), neutropenia (low white blood cell counts), QT prolongation[65], and liver function abnormalities. In rare cases, nilotinib may cause serious side effects, such as sudden death, heart attack, or stroke.

Studies have also shown that particular side effects of taking nilotinib, such as bone and joint pain, fatigue, and nausea, could lead to higher levels of anxiety symptoms in CML patients. Therefore, reducing or alleviating these side effects may not only improve patients' quality of life but also prevent the development of more severe psychological conditions [66].

Researchers have attempted numerous approaches to develop a pharmaceutical formulation that improves solubility, potentially enhancing bioavailability and reducing variability in pharmacokinetics. A wide range of polymer excipients and techniques have been evaluated for their solubilizing properties. These include using nonionic surfactant Tween 20 to increase in absolute bioavailability of nilotinib [67], another technique is to create amorphous nanosuspension which is successfully fabricated using an acid-base neutralization approach with a threefold increase in dissolution and a 36-fold increase in solubility compared to the neat drug [68]. In addition, self-micro-emulsifying drug delivery systems (SMEDDS) have been employed to improve drug release and pharmacokinetic parameters [69].

Furthermore, developing gastro-retentive drug delivery systems (GRDDS) to enhance oral bioavailability by 2.65-8.39-fold compared to Tasigna, a commercially available form of nilotinib. The enhanced bioavailability could offer a pharmacokinetic profile with therapeutic effectiveness for the daily administration of nilotinib, increasing compliance and minimizing side effects [70].

1.5.2 Carvedilol

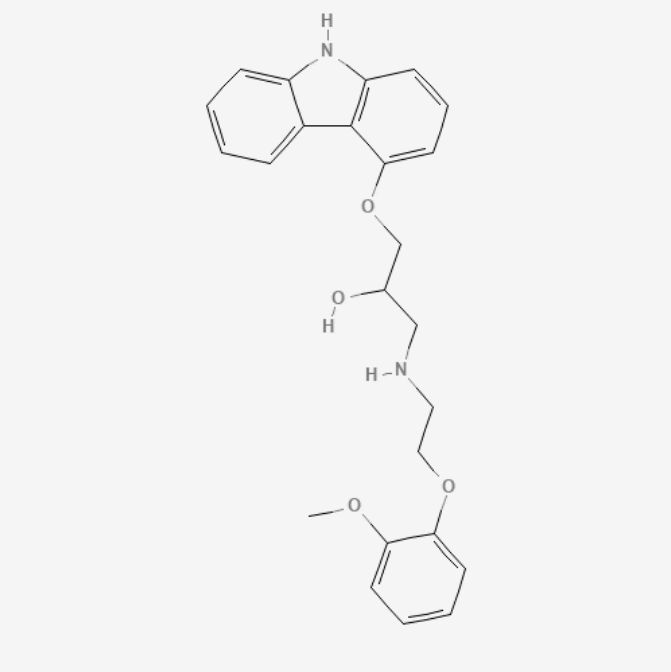

Figure 7: Depicts the chemical structure of Carvedilol, which is also known by its chemical name1-(9H-carbazol-4-yloxy)-3-[2-(2-methoxyphenoxy) ethylamino] propan-2-ol; hydrochloride.

Carvedilol is a third-generation non-selective beta-blocker and α_1-blocker with the capability to inhibit oxidative stress in coronary smooth muscle. Since its introduction, carvedilol has quickly established itself as the standard of care for heart failure management [71] and, It has been approved as the first beta blocker for treating all forms of congestive heart failure, including mild, moderate, and severe conditions, with reduced ejection fraction (HFrEF). Research findings have demonstrated that carvedilol reduces the risk of mortality and hospitalizations related to heart failure by 31% in comparison to a placebo group in patients diagnosed with New York Heart Association class III and IV heart failure, and who have an ejection fraction of less than 25% [72].

It is also approved for managing essential hypertension and left ventricular dysfunction in clinically stable patients following a myocardial infarction (MI). In addition, carvedilol is prescribed off-label for stable angina, atrial fibrillation, prophylaxis against cirrhotic esophageal variceal bleeding, and ventricular arrhythmia [73]. It has also been found to be effective in alleviating tardive movement disorders, psychosis, mania, and depression [74].

Carvedilol is a type of racemic mixture that contains both S(-) and R(+) enantiomers. The S(-) enantiomer acts as a beta adrenoceptor blocker, while the R(+) enantiomer functions as both a beta and alpha-1 adrenoceptor blocker [75,76].

Carvedilol has a molecular weight of 442.9 g/mol and a chemical formula of C24H26N2O4, and molecular structure shown in figure 7. It is a white powder that exhibits high solubility in dimethylsulfoxide, methanol, and methylene chloride. It is also moderately soluble in 94% ethanol and isopropanol, and partially soluble in ethyl ether at room temperature [76]

In aqueous media, carvedilol demonstrates good permeability through the gastrointestinal membrane but is practically insoluble in water, with a solubility of 20 μg/mL at pH 7[77].

Carvedilol is a weak base with a pKa of 7.8 in the pH range of 1-8, It is slightly soluble in simulated gastric fluid at pH 1.0 and its solubility can be increased from 0.01 to 1 mg mL−1 by decreasing pH. As a result of its low aqueous solubility and high permeability, carvedilol can be classified as a class II drug in the Biopharmaceutics Classification System (BCS) [78].

Various polymorphic forms of carvedilol have been identified, including Form I, Form II, Form III, Form IV (hemihydrate), Form V (methyl ethyl ketone solvate), Form VI (ethyl acetate solvate), Form VII, and Form IX (hemihydrate) [8]. Among these forms, Form I is the thermodynamically most stable crystalline form of carvedilol [79].

As stated in the previous paragraph, carvedilol has unique properties that result in a combination of cardiac beta-blockade and peripheral vasodilation, making it a non-selective cardiac beta-blocker with peripheral vasodilating effects. In addition to its antihypertensive effects, carvedilol also exhibits antioxidant properties, reduces neutrophil infiltration, inhibits apoptosis, reduces vascular smooth muscle migration, and improves myocardial remodeling post-acute myocardial infarction.Furthermore, carvedilol has shown promise in the treatment of atherosclerotic disease formation and progression due to its ability to prevent the formation of oxidized low-density lipoproteins and inhibit vascular smooth muscle cell proliferation and migration. Overall, carvedilol's unique mechanism of action and multiple beneficial effects make it a valuable medication in the management of hypertension and cardiovascular diseases [72]. Carvedilol is rapidly absorbed upon administration, with peak plasma concentration (Cmax) within 1 to 2 hours. However, its poor solubility and low dissolution rate may hinder its absorption from the small intestine, resulting in poor oral bioavailability of only 25 – 30%. This poor bioavailability is also due to the high degree of first-pass metabolism.

Carvedilol is a highly lipophilic drug, which allows it to extensively distribute into tissues. It

undergoes metabolism in the liver through oxidation, followed by glucuronidation and conjugation. The metabolism is predominantly mediated by Cytochromes P450, specifically CYP2D6 and CYP2C9.

Carvedilol is generally well-tolerated with a lower frequency of adverse events compared to other beta-blockers, and these events are often dose-related. In a post-marketing surveillance study, only 7% of patients had to discontinue carvedilol due to adverse events. The most common adverse effect is excessive hypotension, manifested as dizziness, fatigue, and headaches, resulting from its vasodilating properties. Other adverse effects related to its beta-blocking properties include dyspnea, bronchospasm, bradycardia, malaise, and asthenia [72].

In the pharmaceutical sector, the development of controlled release dosage forms for oral administration of poorly soluble drugs poses a challenge. This is especially true for drugs with pH-dependent solubility, as the gastrointestinal tract exhibits wide variability in terms of environmental pHs. One approach to overcome this challenge is to increase the dissolution rate of the poorly soluble drug at different pHs, eliminating the pH-dependent solubility, and then controlling its release properties from the pharmaceutical form.

Various techniques have been employed to improve Carvedilol solubility and dissolution rates, including reducing particle size, increasing specific surface area, and stabilizing different forms such as co-crystals[80,81] , self-emulsification, and liquisolid techniques [82] , amorphous solid dispersions [83] , drug-cyclodextrin complex [84] and , chitosan-carvedilol systems [85].Recent advances in nanoscience and nanotechnology have also spurred the development of new carriers with unique properties, such as liposomes, nanocapsules, carbon nanotubes, and naturally occurring nanostructured materials like nanoclays, as efficient platforms for poorly soluble drugs [78,86].

Moreover, recent studies have shown that solidified self-nanoemulsifying drug delivery system (solidified SNEDDS) and surface-modified microspheres, which are lipid-based drug delivery systems, have significantly increased the solubility, dissolution, and oral bioavailability of carvedilol compared to carvedilol powder. These advancements in drug delivery systems offer promising strategies to enhance the solubility and bioavailability of poorly soluble drugs like carvedilol, addressing the challenges associated with their oral administration [87].

1.5.3 Ritonavir

Ritonavir molecule first developed by abbott laboratories in 1992 [88], ritonavir is a peptidomimetic HIV protease inhibitor renowned for its powerful inhibitory effects on the hiv-1 protease enzyme, a critical player in virus replication. Through its ability to hinder this enzyme, ritonavir effectively suppresses the replication of the virus, leading to a decrease in viral load and a deceleration in the progression of the disease. Following saquinavir, ritonavir became the second protease inhibitor approved by the U.S food and drug administration (FDA) in march 1996. Since then, it has been extensively utilized in managing hiv infection under the tradename novir®, demonstrating its significant impact in disease management [89].

Although ritonavir was initially designed to inhibit HIV protease, research has shown that it also inhibits cytochrome P450-3A4, and even in low doses causes a prolongation of the half-life of other protease inhibitors that are metabolized by this pathway. Currently ritonavir is primarily used in combination with protease inhibitors in a low or "booster" dose (50 to 100 mg twice daily) such as atazanavir, fosamprenavir, indinavir, lopinavir, nelfinavir, and saquinavir showing significant virological suppression and better immune outcomes in both treatment-I and treatment-experienced patients [90].

Furthermore, investigations are being conducted to explore ritonavir's potential antiviral activity against other RNA viruses, including coronaviruses. It is being utilized in combination with other medications to treat COVID-19 in individuals who are at high risk of developing severe manifestations of the disease. Moreover, ritonavir has been considered as a therapeutic option for hepatitis C. Additionally, off-label use of ritonavir has been observed in the treatment of specific cancer types, owing to its ability to impede the growth and multiplication of tumor cells. However, extensive clinical trials are necessary to establish more robust and dependable outcomes [89,91].

Ritonavir is characterized as a chiral molecule [92], However, approximately two years after its initial launch in early 1998, certain batches of ritonavir started exhibiting dissolution issues, leading to reports of clinical inefficacy. This situation resulted in a crisis within the market for Abbott Laboratories. Further examination uncovered the presence of a previously unknown new crystalline form, referred to as form II. This new form was found to be thermodynamically more stable than the original form (form I) and exhibited significantly lower solubility (less than 50% soluble compared to form I), consequently leading to the observed poor dissolution behavior in comparison to ritonavir Form I. While both polymorphic forms have an equivalent number of hydrogen bonds, the crystallographic network of hydrogen bonds differs between form II and form I due to the conformational deformation energy disparity [93,94].

The lattice energies of form I indicate a convergence at shorter distances, suggesting its

preferential crystallization at high supersaturation. Both forms exhibit a needle/lath-like crystal habit, with slower growth observed on hydrophobic sides and faster growth on hydrophilic capping habit faces. The aspect ratios of these crystal habits increase sequentially from polar-protic to polar-aprotic and finally non-polar solvents. Surface energies, on the other hand, are higher for form II compared to form I, and they increase proportionally with the polarity of the solvent. The higher levels of deformation, lattice, and surface energies observed in form II are consistent with its lower solubility and subsequent reduced bioavailability[95].

Similar to Nilotinib, ritonavir belongs to the Biopharmaceutics Classification System (BCS) Class IV, characterized by high aqueous solubility and low permeability. It is an L-valine derivative with a molecular weight of 720.95 g/mol and a chemical formula of C37H48N6O5S2. The compound is in the form of a white powder and demonstrates a notable lipophilic nature Due to its sensitivity to light, the protecting amber polyethylene terephthalate bottle serves as a preventive measure, effectively counteracting any potential degradation of the oral solution resulting from exposure to light [96]. It exhibits high solubility in methanol and ethanol, with respective solubilities of 142 mg/ml in DMSO and 100 mg/ml in ethanol. Ritonavir also exhibits some solubility in isopropanol. However, its solubility in water is practically insoluble, estimated to be 1.1x10-4 mg/L at 25 °C [96] .

Ritonavir, characterized by a pKa value of 2.8 and a logP value of 3.9, demonstrates moderate basicity and high lipophilicity. As a result, it exhibits extensive distribution into various tissues upon administration. Binding studies have shown that ritonavir has a high affinity for plasma proteins, particularly albumin and α1-glycoproteins, with a binding capacity of approximately 98% to 99%. The mean blood-to-plasma concentration ratio is 0.6. Interestingly, there is no evidence of saturation of protein binding even at high concentrations of ritonavir. Although the drug shows minimal penetration into the cerebrospinal fluid, the concentration of free ritonavir in the plasma is indicative of its presence in the cerebrospinal fluid.

Metabolism studies using radioactive ritonavir have revealed that its major metabolic pathway in humans aligns with observations made in preclinical studies. The primary enzymes responsible for metabolizing ritonavir are cytochrome P450 enzymes, specifically CYP3A4 and to a lesser extent CYP2D6. Among the metabolites identified in humans, the isopropylthiazole oxidation metabolite (M-2) is the only one detected in the systemic circulation and appears to retain similar activity to the parent compound. The mean plasma half-life of ritonavir is approximately 4 hours. It is primarily eliminated through the hepatobiliary route, with a significant portion of the unchanged drug excreted in feces. After administration of a 600 mg dose of 14C-labeled ritonavir oral solution, 86.4% of the radioactivity was recovered in the feces and 11.3% of the dose was excreted in the urine, consistent with preclinical study findings. The pharmacokinetics of ritonavir display dose-dependent characteristics, as the area under the concentration-time curve (AUC) and maximum plasma concentration (Cmax) increase more

than proportionally with higher oral doses. This implies that the exposure to ritonavir is not directly proportional to the administered dose, necessitating careful consideration of dosage adjustments to achieve optimal therapeutic outcomes [97].

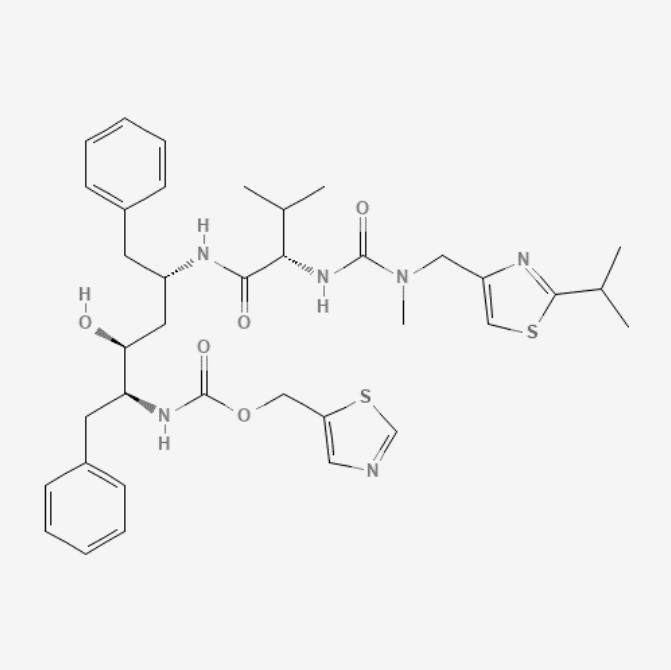

Figure 8: shows chemical structure of Ritonavir. It is also identified by its IUPAC name 1,3-thiazol-5-ylmethyl N-[(2S,3S,5S)-3-hydroxy-5-[[(2S)-3-methyl-2-[[methyl-[(2-propan-2-yl-1,3-thiazol-4-yl) methyl] carbamoyl]amino]butanoyl]amino]-1,6-diphenylhexan-2-yl]carbamate and molecular formula C37H48N6O5S2.

Presently, numerous antiviral agents have been approved for treating viral infections. However, in specific scenarios, the inclusion of a second antiviral agent can offer advantages by providing alternative or combined therapeutic strategies. In this regard, virus-encoded proteases have emerged as promising targets for antiviral intervention. Molecular investigations have elucidated the pivotal role played by viral proteases in the life cycle of diverse viruses. These proteases are responsible for cleaving large polyprotein precursors of the virus, leading to the production of functional viral proteins or the processing of structural proteins necessary for virus assembly.

In the case of HIV, the viral genome consists of three primary genes: gag, pol, and env. Transcription and translation of the gag and pol regions generate precursor polyproteins, namely p55 and p160. Subsequently, the released HIV protease cleaves these polyproteins at multiple sites, resulting in the generation of essential structural and enzyme products. The selectivity of HIV protease inhibitors, such as ritonavir, is achieved through their ability to target specific scissile bonds, including Phe-Pro, Phe-Leu, and Phe-Thr. Ritonavir, a member of the aspartic acid protease family, binds tightly to the active site of HIV-1 protease, which

encompasses distinct subsites for inhibitor interaction. Moreover, ritonavir exhibits significant protein binding, potentially influencing its availability and interaction with the viral target. While the precise correlation between protein binding and clinical efficacy remains uncertain, reductions in antiviral activity in vitro have been observed in the presence of serum proteins like α1-acid glycoprotein. Overall, the mechanism of action of ritonavir as a protease inhibitor offers a valuable approach in the treatment of viral infections, including HIV.Ritonavir is associated with various constitutional side effects, including malaise, dizziness, and insomnia, as well as gastrointestinal symptoms such as nausea, vomiting, abdominal pain, and diarrhea. Metabolic side effects such as hyperlipidemia, hypertriglyceridemia, transaminitis, and rhabdomyolysis can also occur. While reports of QT prolongation have been linked to the use of protease inhibitors, studies have not conclusively established them as independent causes [98]. Due to the metabolic side effects of ritonavir, the addition of lipid-lowering agents may be considered alongside protease inhibitors to mitigate the risk of cardiovascular disease. Additionally, ritonavir has been associated with serious adverse effects including pancreatitis, diabetes mellitus, renal failure, hypersensitivity reactions, Stevens-Johnson syndrome, toxic epidermal necrolysis (TEN), hepatotoxicity, leukopenia, and neutropenia [98].

Cautious use of ritonavir is necessary when co-administered with other medications that inhibit the CYP450-3A4 enzyme, as it can lead to increased levels of drugs in blood serum. Furthermore, patients taking pharmacological agents that act as CYP inducers (e.g., apalutamide, St.'John's wort) should not be given ritonavir, as it can significantly reduce ritonavir plasma concentrations and may result in the loss of virologic response, potential resistance, and cross-resistance [89,99]. Similar to the previously mentioned drugs, Carvedilol and Nilotinib, recent studies have been focused on enhancing the oral bioavailability of ritonavir by improving its solubility and dissolution rate. Various strategies have been investigated to achieve this goal. These include the complexation of ritonavir with cyclodextrin and PVP K30 Soluplus [100] , co-crystallization with co-formers such as citric acid, adipic acid, and amino acids [101,102] and, the application of the solid dispersion technique using Polyvinyl Pyrrolidone (PVP) K-30 [103,104] and, polyethylene glycol 8000 (PEG)[105] .These studies have demonstrated that these approaches can significantly enhance the solubility and dissolution rate of ritonavir, ultimately resulting in improved oral bioavailability.

1.6 High-Performance Liquid Chromatography

Various analytical methods are utilized for the quantification and analysis of samples in colonic drug delivery systems. When selecting an appropriate analytical method, several factors must be considered. These include cost, simplicity, precision, accuracy, reproducibility, and other relevant aspects. It is essential to evaluate these factors prior to conducting the analysis. Additionally, aspects such as the limit of detection (LOD) and limit of quantitation (LOQ) need to be evaluated. The LOD represents the minimum detectable amount of the analyte under specific experimental conditions, while the LOQ indicates the lowest amount of the analyte that can be reliably quantified. It is crucial for the analyte to exhibit stability in solution to ensure reliable analysis of sample solutions. Linearity is another important factor that confirms the validity of the data obtained. Among the employed analytical methods, high-performance liquid chromatography (HPLC) is commonly used in this context [106].

HPLC (High-Performance Liquid Chromatography) is a separation technique used for detecting and analyzing molecules in a sample. The principle of HPLC involves the use of pumps to pass a solvent and the sample through the system under high pressure. The HPLC system comprises various components, including eluting solvents, a pumping system for solvent transfer, an injector for sample introduction, an analytical column for molecule separation, and a detector for signal detection. In HPLC, the solvents used for elution are referred to as the mobile phase, while the column is the stationary phase. The two most common types of HPLC methods are normal-phase and reversed-phase chromatography. In normal-phase chromatography, the mobile phase is non-polar, while the stationary phase is polar. Conversely, in reversed-phase chromatography, the mobile phase is typically a water-organic solvent mixture, with acetonitrile (ACN) or methanol (MeOH) being commonly used organic solvents. The composition of the mobile phase, including the presence of salts and ph adjustments, can be optimized to achieve desired sample elution. The mobile phase composition can be constant throughout the analysis (isocratic method) or changed gradually during the sequence (gradient method). In reversed-phase HPLC, the non-polar stationary phase often consists of silica particles coated with octyl (C8) or octadecyl (C18). The retention of sample molecules on the column is primarily driven by non-polar interactions. The time at which a molecule elutes from the column is known as the retention time (Rt), and it appears as a peak in the chromatogram. Columns come in various lengths, diameters, and particle sizes, and a guard column can be connected to extend the column's lifespan. Overall, HPLC is a powerful analytical method that enables efficient separation and detection of molecules in a sample, offering flexibility in mobile phase composition and column selection to suit specific analytical requirements [107].

The guard column in HPLC contains the same stationary phase material as the analytical

column and serves to protect the analytical column from sample debris and contaminants. Both the analytical column and the detector in HPLC systems can be temperature-controlled. Temperature control can have a positive impact on peak separation and can alter the retention time (Rt) of analytes.

The most commonly used detector in HPLC is the ultraviolet (UV) detector. It operates by measuring the absorption of UV light by the analytes as they pass through the detector cell. UV detection is based on the principle that different compounds have different UV absorption properties, enabling their identification and quantification. Another type of detection method used in HPLC is the charged aerosol detector (CAD). In CAD, the particles in the sample generate the detector signal. The aerosol formed in the detector becomes charged, and the magnitude of charge depends on the particle size and the total charge carried by the aerosol. An aerosol is defined as a mixture of solid particles and/or liquid droplets suspended in a gas. The CAD detector utilizes a nebulizer to break the liquid stream into small droplets, achieved by a high-velocity gas flow. The typical gas source used for the CAD detector is nitrogen. In the upcoming chapters, detailed explanations will be provided regarding the various HPLC methods employed for specific drugs in the study. This comprehensive discussion aims to offer a comprehensive understanding of the specific techniques used for analyzing each drug [107], [108]. A schematic illustration of the HPLC system is shown in figure 9.

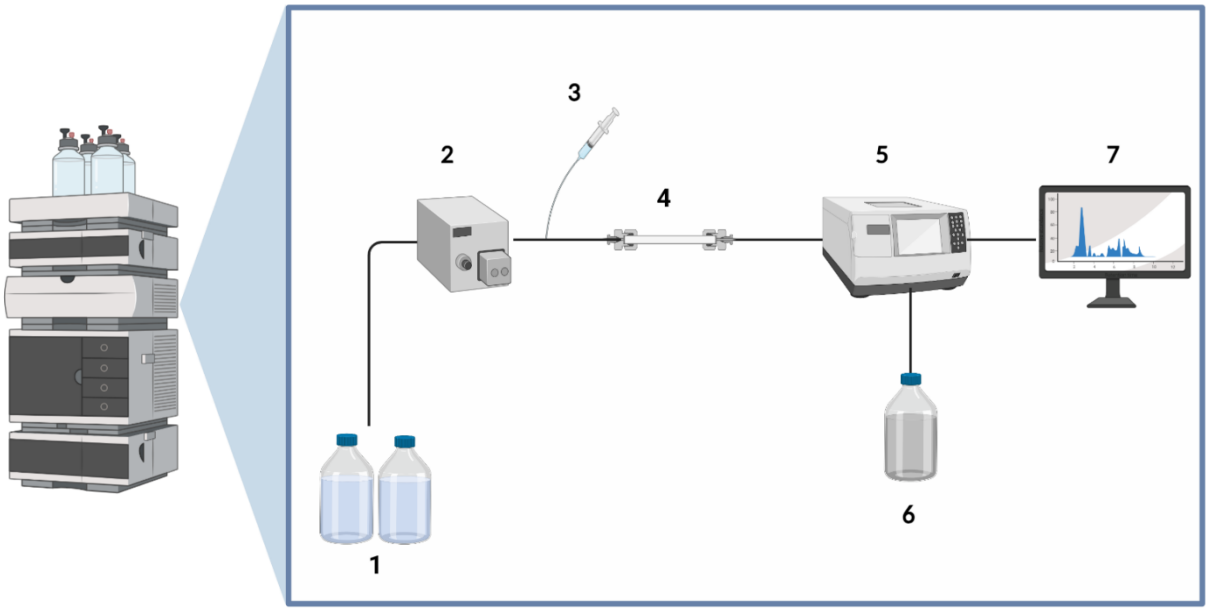

Figure 9: A schematic illustration of the HPLC system. 1) expresses the mobile phases, 2) expresses the pump, 3) expresses the injector for injecting the sample, 4) expresses the analytical column, 5) expresses the detector, 6) expresses the waste container, and 7) expresses the experimental data shown in the computer software. Created with BioRender.com

2 Aim of Study and Hypothesis

The objective of this study was to explore the impact of proteins present in fasted state simulated colonic fluid on various compounds exhibiting diverse physicochemical and plasma protein binding properties. The influence was assessed by measuring the apparent drug solubility of three selected compounds specifically nilotinib, carvedilol and ritonavir. Effect of three protein sources, namely bovine serum albumin, porcine gastric mucin type II, and porcine intestinal mucus, were investigated. The findings from this study will provide valuable knowledge and contribute to the advancement of pharmaceutical sciences in the field of colonic drug delivery. The hypothesis underlying this study is that increased concentration of three different proteins affects the apparent solubility of three specific drugs, each possessing distinct physicochemical properties, in fasted state simulated colonic fluid. By investigating these interactions, we aim to elucidate the influence of proteins on drug solubility in a simulated colonic environment, thus contributing to a deeper understanding of the factors influencing drug behavior in the colon during fasting conditions.

3 Experimental Part

3.1 Material and Methods

Tris(hydroxymethyl)aminomethane (TRIS), bile bovine, cholesterol, sodium hydroxide (NaOH), linoleic acid, palmitic acid, bovine serum albumin (BSA), gastric porcine mucin type II, potassium dihydrogenphosphate (KH_2PO_4), Sodium phosphate (Na_3PO_4), Trifuoroacetic acid (TFA), maleic acid disodium salt 99%, hydrochloric acid (HCI), dichloromethane (DCM), orthophosphoric acid 85%, MeOH, ACN, isopropanol and ethanol purchased from VWR (Fontenay-sous-Bois, France). PhosphatidyIcholine from soybean (phospholipids) purchased from Lipoid GmbH (Ludwigshafen am Rhein, Germany). Carvedilol purchased from Alfa Aesar (Product number C2260, Lancashire, UK). Ritonavir purchased from BASF (Ludwigshafen am Rhein, Germany). Nilotinib hydrochloride monohydrate (Nilotinibi hydrochloridum monohydricum) purchased from UNIKEM (Copenhagen V, Denmark). Milli-Q water (MQ water) was obtained from a Milli-Q water purification system using a SG Ultra Clear 2002 from SG Wasseraufbereitung und Regenerierstation GmbH (Barsbüttel, Germany).

3.2 Fasted State Stimulated Colonic Fluid

The composition of the biorelevant media FaSSCoF is presented in Table 3.

Table 3: The composition of FaSSCoF.

Chemical	**Concentration**
Tris	45 mM
Maleic acid	76 mM
Bile bovine	0.15 mM
Phospholipids	0.3 mM
Palmitic acid	0.1 mM
Ad MQ water	
NaOH ≈ pH 7.8	

To prepare the 1 L FaSSCoF solution, the following steps were taken: Initially, approximately 800 mL of MQ water was added to a 1000 mL beaker. Then, precise measurements of 5.45 g of TRIS, 12.16 g of maleic acid, and 0.113 g of bile bovine were obtained and added to the water in the beaker. To facilitate dissolution, a magnet was positioned at the bottom of the beaker, and the contents were stirred using a magnetic stirrer until completely dissolved. Next the pH of the solution was adjusted to a value of 7.8 using NaOH. This was achieved by employing a pH meter (Sension+ PH31 from Hach, Loveland, Colorado, USA). Subsequently, the solution was transferred to a 1000 ml volumetric flask, and MQ water was added until the solution reached the marked line on the flask.

In separate 20 mL glass vials, 0.222 g of phospholipids and 0.026 g of palmitic acid were accurately weighed and dissolved in 2.5 mL of DCM. Afterwards, approximately 400 mL of the prepared solution from the previous step was transferred to a round bottom flask containing the dissolved phospholipids and palmitic acid in DCM.

To remove the DCM solvent, the round bottom flask was placed in a rotary evaporator with a water bath set at a temperature of 41°C and a pressure of 700 mbar. The evaporation process lasted for 15 minutes using a Büchi® Rotavapor® R-210 evaporator equipped with a Büchi@ Vacuum Controller V-850, Büchi@ Vacuum Pump V-100, and a Büchi@ Distillation Chiller B-741 from Holm and Halby (Brondby, Denmark).

Finally, the two solutions, previously prepared and now combined, formed the final FaSSCoF solution. This solution was stored in a heating cabinet with a temperature of 37°C and maintained under constant magnetic stirring. The FaSSCoF solution remained viable for at least 48 hours.

Various protein sources were introduced into the FaSSCoF solution. Volumetric flasks were prepared with different concentrations of Bovine Serum Albumin (BSA) and Porcine Gastric Mucin Type II, specifically 3 mg/mL, 9 mg/mL, and 15 mg/mL respectively. These protein compositions were added to each flask and dissolved in the FaSSCoF solution. Afterward, the flasks with the different protein compositions were stored in the heating cabinet at a temperature of 37 °C while being subjected to magnetic stirring.

The protein concentration of the porcine intestinal mucus (PIM) was determined during the mucus characterization process (1.3.2). To prepare different compositions with protein concentrations of 3 mg/mL, 9 mg/mL, and 15 mg/mL, the appropriate amount of PIM was weighed and dissolved in FaSSCoF solution. Magnetic stirring was employed during the dissolution process, which took place at a temperature of 37 °C. All experiments involving the assessment of apparent solubility were carried out on the same day that the mucus was thawed and dissolved in FaSSCoF.

3.3 Mucus Collection

The collection involved obtaining porcine intestinal mucus (PIM) from a 37 kg pig at the Department of Experimental Medicine, University of Copenhagen, Panum, Denmark. The mucus was extracted from the small intestine of a pig that had undergone a 20-hour fasting period. Prior to handling the intestine, a fume hood was sterilized and equipped with necessary tools, paper, and storage containers. Additionally, a Styrofoam box filled with ice and bags for transportation was prepared. The intestine was divided into smaller sections and dissected open using surgical scissors. The mucus was carefully scraped off using an objector glass typically employed in microscopy. The collection of mucus was completed within 2 hours after the dissection and stored in sealed sterilized plastic containers and Eppendorf tubes.. The samples were separately stored in sealed sterilized plastic containers and Eppendorf tubes and kept in a laboratory freezer at -20 °C.

3.4 Apparent Solubility Evaluation

To evaluate the solubility of each drug, powdered forms of the drugs were added to 20 mL vials in triplicates. The exact weight of the drugs was not critical, but it was essential to ensure an excess amount of drug in each vial to make sure we have saturated maximum protein binding capacity of the solution. A single magnet was placed in each vial containing the drug compound. Additionally, FaSSCoF with different concentrations of proteins (0,3,9,15 mg/ml) were added to the vials. For standardization, triplicate vials of each drug compound with FaSSCoF and no added protein was included. The set of 12 vials, representing drug in different concentration of protein, were then stored in a heating cabinet at a constant temperature of 37°C while being subjected to magnetic stirring.

To maintain physiological pH levels, the pH of each compound was checked using a pH meter (Sension+ PH31 from Hach, Loveland Colorado, USA), and if required, corrections were made using hydrochloric acid (HCI) or sodium hydroxide (NaOH). Throughout the solubility study, samples were collected at regular intervals. For most of the samples, the intervals were set at 1, 2, 4, 6, 8, 24, and 48 hours. However, for samples involving FaSSCoF compositions with porcine intestinal mucus (PIM), the intervals were adjusted to 1, 2, 4, 6 and 8 hours because these sample were more prone to microbial contamination.

For each sample, 1000 µL was transferred to an Eppendorf tube, which was then subjected to centrifugation for 30 minutes at 13,300 rounds per minute (RPM) (17,000 rcf). The centrifugation process was conducted using a Sorvall™M Legend™M Micro 21R microcentrifuge from Thermo Fisher Scientific (Osterode, Germany) and maintained at a

temperature of 37°C. Following centrifugation, 100-200 µL of the supernatant was carefully transferred to a new Eppendorf tube and diluted with 100-200 µL of an organic solvent, either acetonitrile (ACN) or MeOH, based on the solubility properties of each compound.

The Eppendorf tube with the diluted sample was then centrifuged again for 15 minutes at 13,300 RPM (17,000 rcf). After the final centrifugation, 100 µL of the supernatant was transferred to a 400 µL insert within a 2 mL vial.

Subsequently, each sample was analyzed using an analytical High-Performance Liquid Chromatography (HPLC) method described in detail for each drug in chapter (4.4). An illustration of the sampling process for apparent solubility is provided in Figure 10.

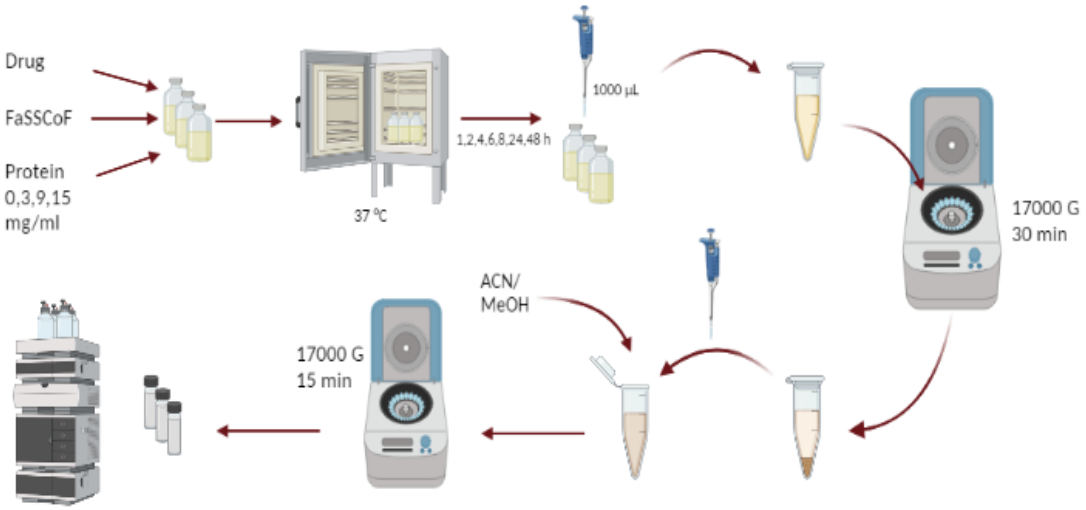

Figure 10: This figure depicted a visual representation of the methodology employed to determine apparent drug solubility for compounds in excess within various FaSSCoF compositions. FaSSCoF compositions and vials are maintained in a heating cabinet at a constant temperature of 37 °C. After specific time intervals of 1,2,4,6,8,24, and 48 hours, a 1000 µL sample is collected from each vial and transferred to an Eppendorf tube. Subsequently, centrifugation is performed for 30 minutes at a force of 17000 G.The supernatant resulting from the centrifugation is then diluted with an appropriate organic solvent (either ACN or MeOH). The newly prepared Eppendorf tube with the diluted sample is subjected to a second round of centrifugation for 15 minutes at a force of 17000 G. Finally, the supernatant is carefully transferred to an HPLC vial and subjected to analysis using RP-HILC-UV. Created with BioRender.com.

3.5 Analysis of Samples

The solubility samples of the investigated compounds in various FaSSCoF compositions were subjected to analysis using the reversed-phase high-performance liquid chromatography with ultraviolet detection (RP-HPLC-UV) method. The analysis was carried out using a Dionex Ultimate 3000 pump, Dionex Ultimate 3000 Autosampler, Dionex Ultimate 3000 column compartment, and a Diode Array Detector (Thermo Scientific, Waltham, Massachusetts, USA). Given the very low solubility of all three compounds in aqueous solutions, it was crucial to develop an HPLC method with sufficient LOD. The method developed in this study for the detection of Nilotinib offers the advantage of detecting our desired limit of quantification (LOD) of 0.0156 µg/mL, along with a short analysis time of 19 minutes for each sample of nilotinib. Detailed explanations of the different RP-HPLC-UV methods for each compound can be found in Chapter (4.4.1-3).

3.5.1 RP-HPLC-UV method for Nilotinib

Based on physicochemical properties of nilotinib , developing an optimal reversed-phase liquid chromatography method for separating nilotinib presents a challenge, requiring the establishment of a sensitive high-performance liquid chromatography (HPLC) method to accurately quantify low concentrations.

Prior to analysis, careful sample preparation was crucial to ensure precise and reproducible results. The solubility samples of nilotinib were dissolved in acetonitrile and filtered through a 0.45 µm membrane filter to eliminate any particulate matter. Special care was taken to maintain the integrity and stability of nilotinib during sample preparation. While the stability of nilotinib under various conditions has been evaluated in previous studies, our present study, all steps were conducted under dark conditions.

The HPLC analysis was performed using a Dionex Ultimate 3000 system equipped with a reverse-phase C18 column ACE EXCEL 5, C18, 100 mm x 4.6 mm , 5 µm column (Aventor, Radnor, Pennsylvania, USA). The selected mobile phase consisted of a 1.36 g/L solution of potassium dihydrogen phosphate-buffered solution (pH = 2, adjusted with phosphoric acid) as mobile phase A, along with a mixture of mobile phase A and acetonitrile [20:80 V/V] as mobile phase B. Flow rate was set to 0.8 $mL \cdot min^{-1}$. Solvents were freshly prepared and degassed by ultrasonication for 15 min for each series of analysis. The column used was maintained at 40°C. The injection volume was 10 µL, and the eluents were monitored at a wavelength of 240 nm. The retention time for nilotinib was found to be approximately 12-13 min. The total run time for each analysis was 19 minutes. The gradient flow of the Nilotinib HPLC method is

mentioned in Appendix A.

To construct the calibration curve, stock solutions of nilotinib (1 mg/mL) were prepared in ACN and stored in the dark. On each analysis day, a series of standard solutions with known concentrations of nilotinib were freshly prepared by diluting the stock solutions.

The linearity of the calibration curve was of utmost importance, it indicates that as the concentration of nilotinib increases, the area of each peak should increase proportionally, as shown in Figure 11. The linearity was assessed by evaluating the correlation coefficient (R^2) obtained from a linear regression analysis of the data points. An R^2 value close to 1 suggests high linearity, indicating the HPLC method's capability to accurately quantify nilotinib over a wide concentration range.

The sensitivity of the method was evaluated using the detection limit (LOD) and the lower limit of quantification (LLOQ). Determining the LOD involves statistical analysis and experimental determination. Typically, a series of Nilotinib solutions with progressively lower concentrations, well below the expected quantifiable range, is analyzed.

To accurately determine the LOD, multiple replicate measurements are performed at each concentration level to account for variability. The LOD is then calculated using statistical methods such as standard deviation calculations or regression analysis.

In this study, the developed method achieved an LOD of 0.0156 µg/mL, enabling the determination of Nilotinib concentrations even in samples with very low Nilotinib concentrations.

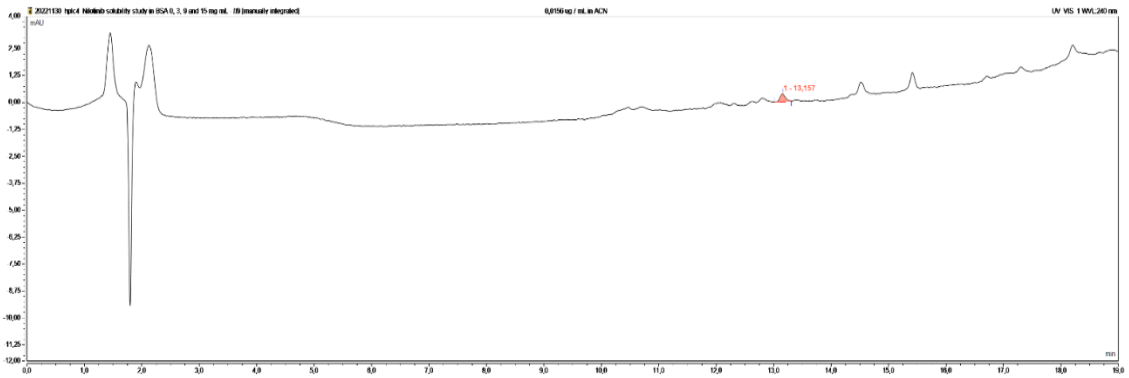

Figure 11: Chromatogram for lowest detectable concentration of Nilotinib with 0.0156 µg/mL.

3.5.2 RP-HPLC-UV method for Carvedilol

The determination of Carvedilol content has been accomplished through various analytical methods, including High-performance liquid chromatography (HPLC) with fluorescence detection[110,111], mass spectrometry, and electrochemical detection [112]. Additionally, the application of capillary electrophoresis for the quantification of Carvedilol has been reported [113]. In this study, our objective was to employ the HPLC method as it offers a simple, rapid, reproducible, and cost-effective approach for quantifying Carvedilol content in our samples. Moreover, this method has been previously validated in other studies [114], undergoing rigorous quality control and accuracy assessment. Although some modifications were made to align the method with our specific laboratory equipment, its overall reliability and efficacy remained intact.

The determination of drug content from samples was conducted using High-performance liquid chromatography (HPLC) equipped with an Ultimate 3000 Ultraviolet (UV) detector, UltiMate 3000 autosampler, and UltiMate 3000 pump from Thermo Scientific (Waltham, MA, USA). For the chromatographic separation, an XTerra Shield RP18 Column with dimensions of 4.6 mm x 150 mm and particle size of 5 µm, manufactured by Waters (Milford, Massachusetts, USA), was employed under controlled temperature 25°C.

Considering the solubility and chemical properties of the drugs, the mobile phase consisted of a mixture of 0.1% Trifluoroacetic acid (TFA) in Acetonitrile (ACN) and a 10 mmol/L sodium phosphate solution at pH 2, with a ratio of 40:60, respectively. The pH of the mobile phase was adjusted to 2 using 1 M hydrochloric acid. Prior to use, the mobile phase was filtered through a 0.45 µm membrane filter paper and degassed using ultrasonication for 15 minutes.

During the analysis, a sample injection volume of 10 µL was used, and the flow rate was set at 1.0 ml/min. The effluent from the column was monitored at a wavelength of 210 nm using the UV detector. The injection time for each sample was 5 min and the retention time of the Carvedilol was determined to be 2.75±0.03 minutes. A standard stock solution of carvedilol with a concentration of 1 mg/ml was prepared by dissolving 25 mg of the drug in 25 ml of Acetonitrile (ACN) in a calibrated flask. From this stock solution, standard samples with a concentration range of 0.156 µg/ml to 50 µg/ml were prepared by diluting with Acetonitrile (ACN).

Calibration curves were constructed by plotting the peak area of carvedilol against its concentration, and these curves exhibited linearity within the concentration range of 1-35 µg/ml. The limit of detection (LOD) and limit of quantification (LOQ) for the high-performance liquid chromatography method were determined to be 0.156 µg/ml and 0.85 µg/ml, respectively. The resulting standard curve, is presented in appendix chapter.

3.5.3 RP-HPLC-UV method for Ritonavir

In the realm of Ritonavir analysis, a thorough exploration of existing literature reveals that this compound has been extensively evaluated using a range of analytical methodologies, such as spectrophotometry methods [115], RP-HPLC methods [116], [117] and, HPTLC [118]. Notably, Ritonavir exhibits exceptional hydrophobic properties, rendering it non-ionizable and demonstrating prolonged retention in reverse phase chromatography [119]. Given the paramount importance of accurate quantification, there is a pressing need to establish an HPLC method that not only exhibits high sensitivity but also facilitates rapid quantification, particularly in the context of pharmaceutical formulations. Moreover, With the widespread adoption and FDA approval of Ritonavir for the treatment of COVID-19, researchers are increasingly interest in the development of greener analytical methods that can effectively determine Ritonavir concentration, thereby minimizing ecological repercussions and enhancing the well-being of analysts involved in its assessment [120].

Various analytical methods have been documented for the quantitative analysis of Ritonavir, both individually and in combination with other drugs in biological samples and formulations. In the present study, a highly sensitive, precise, and accurate method was employed, which proved effective in reliably quantifying the active pharmaceutical ingredient (API) content. The method underwent statistical validation following the guidelines set by the International Conference on Harmonization (ICH) with respect to specificity, linearity, accuracy, precision, and robustness, along with recovery studies[121]. To conduct the analysis, an Ultimate 3000 Ultraviolet (UV) detector, UltiMate 3000 autosampler, and UltiMate 3000 pump from Thermo Scientific (Waltham, MA, USA) were utilized. The chromatographic separation was achieved using an ACE Excel 5 C18-AR column (100 mm length, 4.6 mm internal diameter, and 5 µm particle size) from Aventor (Radnor, Pennsylvania, USA).

The mobile phase, consisting of Acetonitrile and MilliQ water in a 50:50 (v/v) ratio, was freshly prepared and degassed by sonicating it for 15 minutes prior to use, Similarly, as done for the analysis of other drugs. The column and HPLC system were maintained at a temperature of 30°C, and the column was equilibrated for a minimum of 30 minutes prior to start analysis, allowing the mobile phase to flow through the system. the flow rate was set at 0.8 mL/min, with injection volume of 10 µL, and the detection wavelength was set at 210 nm with a runtime of 9 minutes, resulting in well-shaped peaks for Ritonavir, which were well-separated at retention times of 7.2-7.4 minutes.

Before the HPLC analysis, the solubility samples were diluted with isopropanol. The diluted solution was then filtered through a 0.45-µm membrane filter and used for the assay. For the preparation of the stock solution, an accurately weighed sample of 100 mg of Ritonavir was

transferred into a 100 mL volumetric flask. Subsequently, working standard solutions were prepared by repeated dilution of the stock solution in the range of 500-0.25 µg/mL.
The linearity of the calibration curve was observed within the concentration range of 50-0.25 µg/mL and is presented in Figure 20.

3.6 Data Analysis

All experiments for apparent drug solubility were performed in triplicates. The data obtained from the solubility studies were analyzed using Microsoft Excel (Version 2022, Microsoft, Redmond Washington, USA) for data organization, graph construction, and basic statistical analysis. Additionally, simple linear regression analysis was performed to explore any correlations between apparent drug solubility and relevant parameters. These analyses and software tools were essential in interpreting the solubility data and providing valuable insights into the effects of proteins on drug solubility in fasted state stimulated colonic fluid.

4 Results

This thesis has successfully determined the apparent drug solubility of three compounds using various compositions of FaSSCoF. The impact of protein concentration on the apparent drug solubility was analyzed, and the results for BSA, mucin, and PIM protein sources are presented in Figures 12-14.

Furthermore, a linear regression analysis was performed on the slopes obtained from the investigation of increased protein concentration in FaSSCoF media for the protein sources BSA, mucin, and PIM. The detailed results of this analysis can be found in Appendix (C).

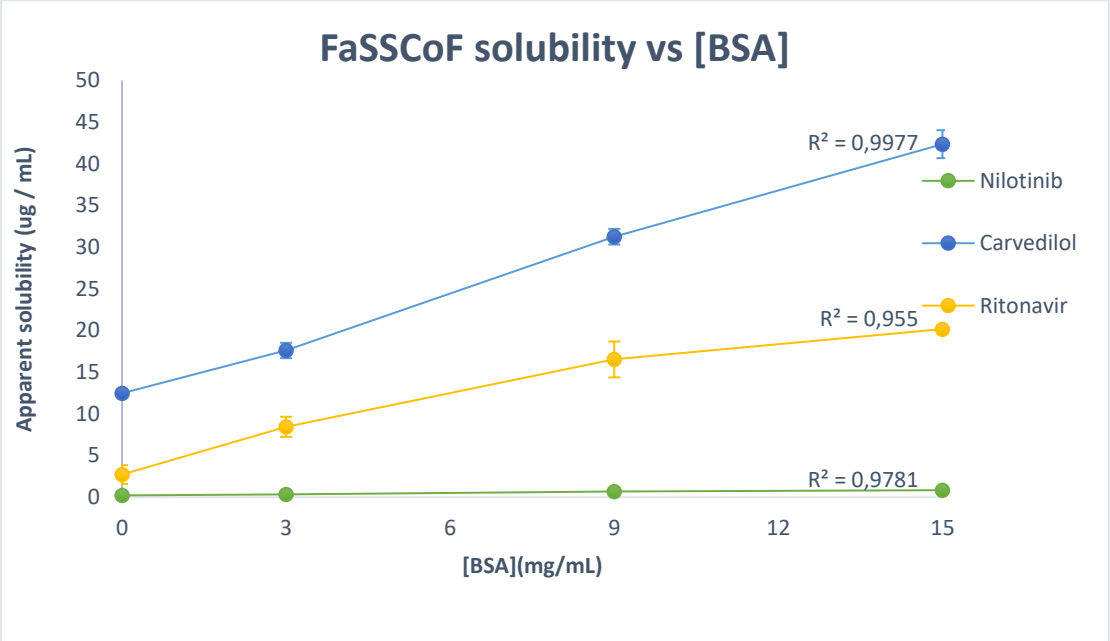

Figure 12: Illustrates the relationship between apparent drug solubility and protein concentration for BSA at concentrations of 0, 3, 9, and 15 mg/mL. The apparent drug solubility values were determined for Nilotinib, Carvedilol,Ritonavir, with a sample size of six replicates (n=6). The error bars represent the standard deviation (± SD) of the data points.

In the presence of BSA in the FaSSCoF medium, the apparent drug solubility of all invested compounds increased. Furthermore, there is a relationship between an increase in perceived drug solubility and increasing the concentration of BSA. For all three compounds, a near-linear relationship between apparent drug solubility and increased BSA concentration was observed. The linearity was determined by calculating the correlation coefficient (R^2) using a linear regression analysis of the data points. An R^2 value close to one indicates high linearity, indicating that the apparent solubility of our medications increases linearly with increasing BSA concentration.

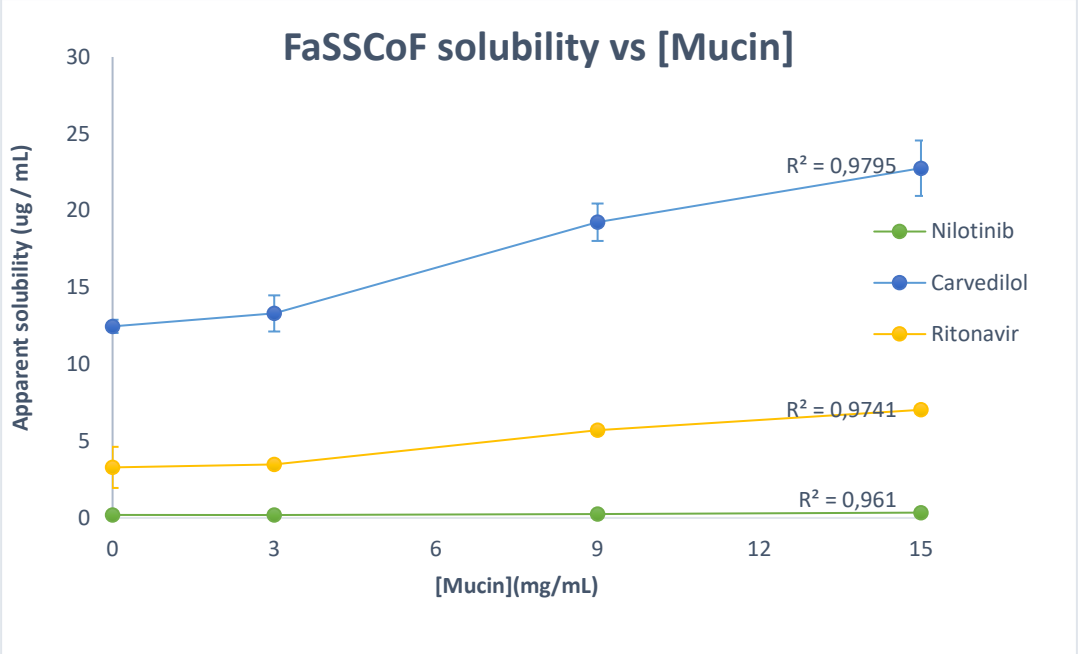

Figure 13: illustrates the apparent drug solubility for Nilotinib, Carvedilol and Ritonavir as a function of the protein concentration of 0, 3, 9, and 15 mg/mL mucin. accordingly (n=6). The error bars represent the standard deviation (± SD) of the data points.

The results show that when the concentration of mucin was increased, there was an observed increase in the apparent solubility of all three compounds (Nilotinib, Carvedilol, and Ritonavir). Furthermore, a near-linear correlation was observed between the increased mucin concentration and the apparent drug solubility.

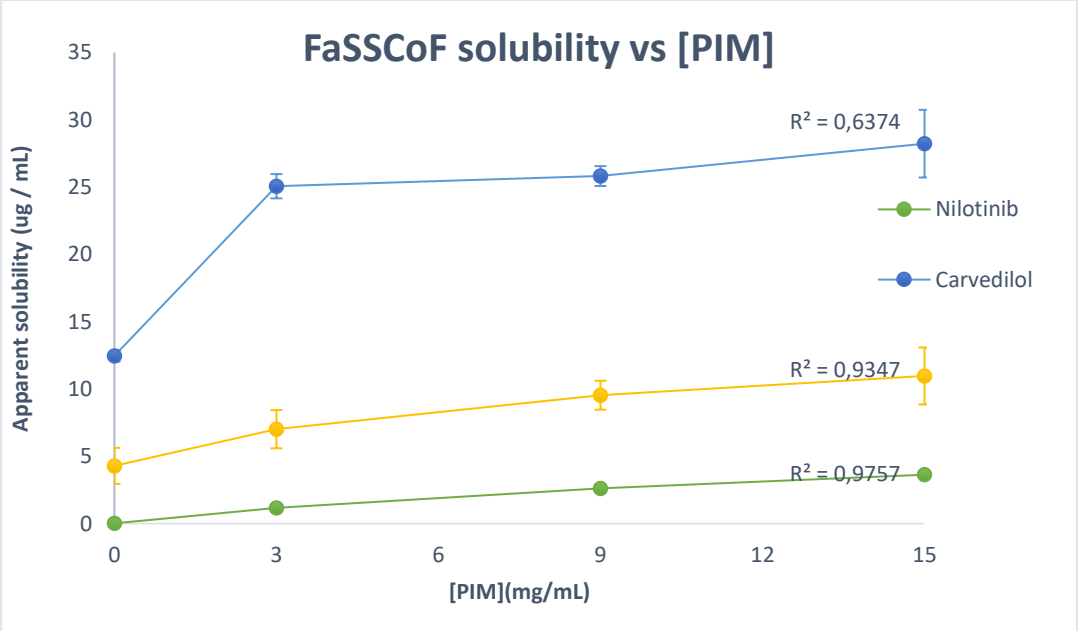

Figure 14: illustrates the apparent drug solubility for Nilotinib, Carvedilol and Ritonavir as a function of the protein concentration of 0, 3, 9, and 15 mg/mL PIM. accordingly (n=6). The error bars represent the standard deviation (± SD) of the data points.

Similar to the influence of BSA and Mucin, the apparent drug solubility increased in the presence of PIM as a protein source for all three compounds. A close to linear correlation was found between the apparent drug solubility and the increased concentration of PIM for Nilotinib and Ritonavir. However, no linearity was observed for the apparent solubility of Carvedilol with an increase in PIM concentration. The R^2 values are provided in Appendix C.

These results demonstrate that both the concentration of protein and the choice of protein source have an impact on the apparent drug solubility of compounds with varying physicochemical properties in FaSSCoF. In the following chapter, we will discuss in more detail the specific effects of these proteins on each individual compound.

5 Discussion

5.1 Nilotinib

The solubility of Nilotinib, a drug compound, in FaSSCoF containing various protein sources, namely BSA (Bovine Serum Albumin), mucin, and PIM (Porcine Intestinal Mucin), was investigated. Several HPLC-UV methods have been published for the quantification of nilotinib but have limited applicability in clinical routine due to the requirement of expensive solid-phase-extraction or additional apparatus set up for sample preparation (e.g., enrichment column, exchange after 50 injections) [109]. Moreover, these methods have longer run times, approximately 30 minutes, which are not suitable for our experiment involving 84 samples per run excluding standard samples.

A robust and sensitive HPLC method was successfully developed for the analysis of nilotinib in solubility samples. The method demonstrated precise and accurate quantification, even at low concentrations It was observed that the presence of all three protein sources led to an increase in the apparent solubility of Nilotinib, with PIM having the highest influence, followed by BSA, and mucin showing the lowest effect.

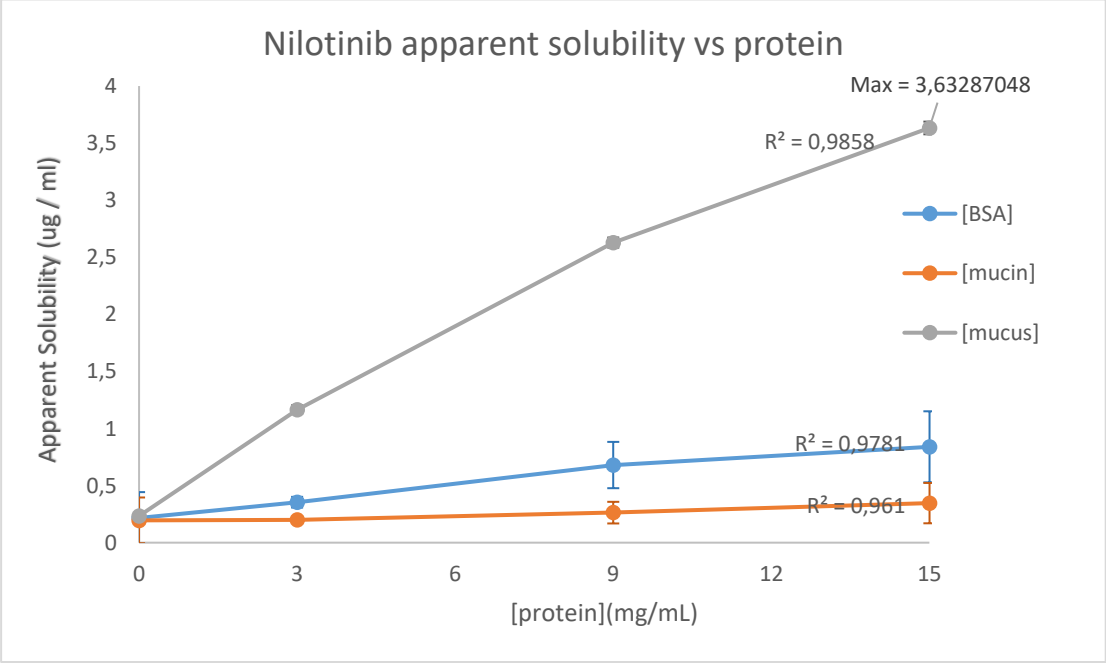

Figure 15: The apparent drug solubility as a function of protein concentration for Nilotinib in FaSSCoF as solvent (n=6). Maximum Apparent solubility value has been mentioned on the graph. Data shown with ± standard deviation.

A nearly linear relationship between protein concentration and increased solubility was observed, as the solubility of Nilotinib increased with higher protein concentrations of 0 mg/mL, 3 mg/mL, 9 mg/mL, and 15 mg/mL. The FaSSCoF compositions containing 15 mg/mL protein exhibited the highest apparent drug solubility with the value of 3.63 ug/ml . This relationship is depicted in Figure 15.

Previous studies have demonstrated that the addition of BSA to poorly soluble compounds can enhance their solubility. Remarkably, even a low concentration of 0.5% BSA in an aqueous buffer system was found to significantly increase drug solubility [122,123].

Interestingly, a previous study conducted by the Physiological Pharmaceutical Group at the Department of Pharmacy, University of Copenhagen, demonstrated a decrease in apparent drug solubility when influenced by mucin in compounds with the highest apparent drug solubility in FaSSCoF, such as mesalazine, naproxen, sulfasalazine, and sulindac.

Mucin proteins, on the other hand, have a structural tendency to aggregate. The mucin molecule possesses regions that are both lipophilic (attracted to lipids) and lipophobic (repelled by lipids), allowing for the formation of hydrogen bonds and electrostatic interactions. These interactions may increase the likelihood of mucins aggregating and engaging in adhesive interactions with other compounds [42].

The variation in the observed drug solubility between mucin and PIM could be attributed to other factors, such as presence higher amount of bile salts, fatty acids, and phospholipids in the FaSSCoF solution with PIM. Furthermore, it is worth considering whether the physicochemical properties of the compounds exhibit similarities that could account for the behavior observed in relation to the protein source and protein binding.

5.2 Carvedilol

The obtained results from our study on the solubility of Carvedilol in FaSSCoF formulation incorporating various protein sources showed that Bovine Serum Albumin (BSA) demonstrated the most significant impact on the apparent solubility of Carvedilol, followed by mucus, while mucin exhibited the least effect. These findings are different to our previous study on Nilotinib, where we observed that mucus had the highest impact on its solubility. Similar to Nilotinib we identified relationship between increase protein concentration and increased solubility, as the protein concentrations in the formulation increased from 0 mg/mL to 15 mg/mL, Carvedilol's solubility displayed a positive correlation. Therefore, the FaSSCoF compositions containing 15 mg/mL BSA exhibited the highest levels of apparent drug solubility, specifically reaching 42.356 µg/mL. The only exception is that there is no linear correlation between the

concentration of mucus and the apparent solubility of Carvedilol. This relationship is illustrated in Figure 16.

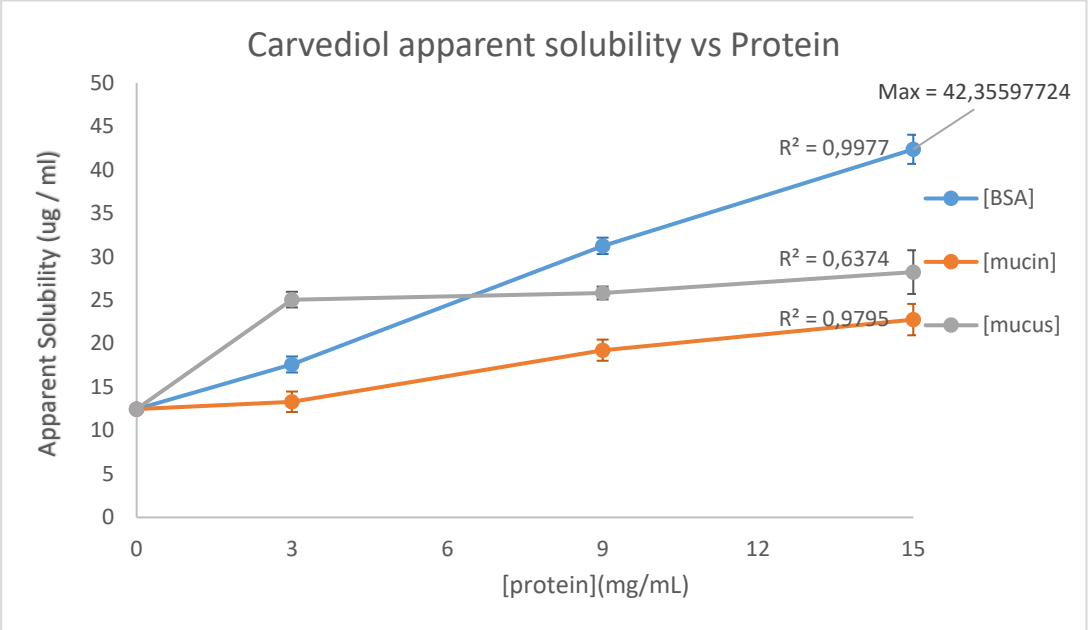

Figure 16: The apparent drug solubility as a function of protein concentration for Carvedilol in FaSSCoF as solvent (n=6). Maximum Apparent solubility value has been mentioned on the graph. Data shown with ± standard deviation.

These contrasting results can be attributed to several factors. Firstly, BSA, being a highly abundant protein with a well-known solubilizing effect in-vivo, may possess specific binding sites that interact favorably with Carvedilol molecules, promoting their solubility in the FaSSCoF formulation. BSA's ability to form complexes with hydrophobic compounds like Carvedilol could enhance its solubility to a greater extent. On the other hand, mucus, with its complex structural characteristics, might contribute differently to the solubility of carvedilol The presence of lipophilic and lipophobic regions within mucin molecules may result in variable interactions with carvedilol, influencing its solubility. These interactions could involve hydrogen bonding, electrostatic interactions, or even aggregation phenomena, leading to a different solubilizing effect compared to BSA. Furthermore, it is worth noting that the specific physicochemical properties of Carvedilol and Nilotinib, including their molecular structure, lipophilicity, and potential binding sites, might also play a role in determining the differential impact of protein sources on their apparent solubility in the FaSSCoF formulation. These properties can influence the strength and nature of interactions between the proteins and the drug molecules, affecting their solubility behaviors. The differences in solubility patterns observed between Carvedilol and Nilotinib may arise from the distinct combination of these physicochemical properties in each drug, contributing to the varying effects of BSA and mucus on their solubility in FaSSCoF.

5.3 Ritonavir

The results obtained from the solubility studies of Ritonavir in a FaSSCoF formulation, incorporating similar protein such as BSA, mucin, and PIM, yielded expected outcomes based on the results obtained from previous compounds. BSA demonstrated the highest impact on the apparent solubility of Ritonavir, followed by mucus, while mucin exhibited the lowest effect. These outcomes align with the observations from our previous study on Carvedilol, where BSA also exerted the highest impact on solubility. Interestingly similar to Nilotinib and Carvedilol, a correlation was identified between protein concentration and the apparent solubility of Ritonavir. As the protein concentrations in the formulation increased from 0 mg/mL to 15 mg/mL, Ritonavir's solubility displayed a near-linear correlation. Consistent with the trends observed for both Nilotinib and Carvedilol, the FaSSCoF compositions containing 15 mg/mL protein exhibited the highest levels of apparent drug solubilities for Ritonavir as well. Specifically, Ritonavir achieved a significant apparent solubility of 20.1675 µg/mL with 15 mg/mL of BSA. Notably, unlike Carvedilol, there was no exception regarding the correlation between the concentration of mucus and the apparent solubility of Ritonavir. The relationship between mucus concentration and solubility remained linear, consistent with the overall trend observed for all protein sources. These findings demonstrate that Ritonavir shares similar behavior with the two other tested drugs, Nilotinib and Carvedilol, despite having its own distinct physicochemical properties. Moreover, these results provide valuable insights into the solubility behavior of Ritonavir in the FaSSCoF formulation, contributing to our understanding of its formulation development and potential optimization.

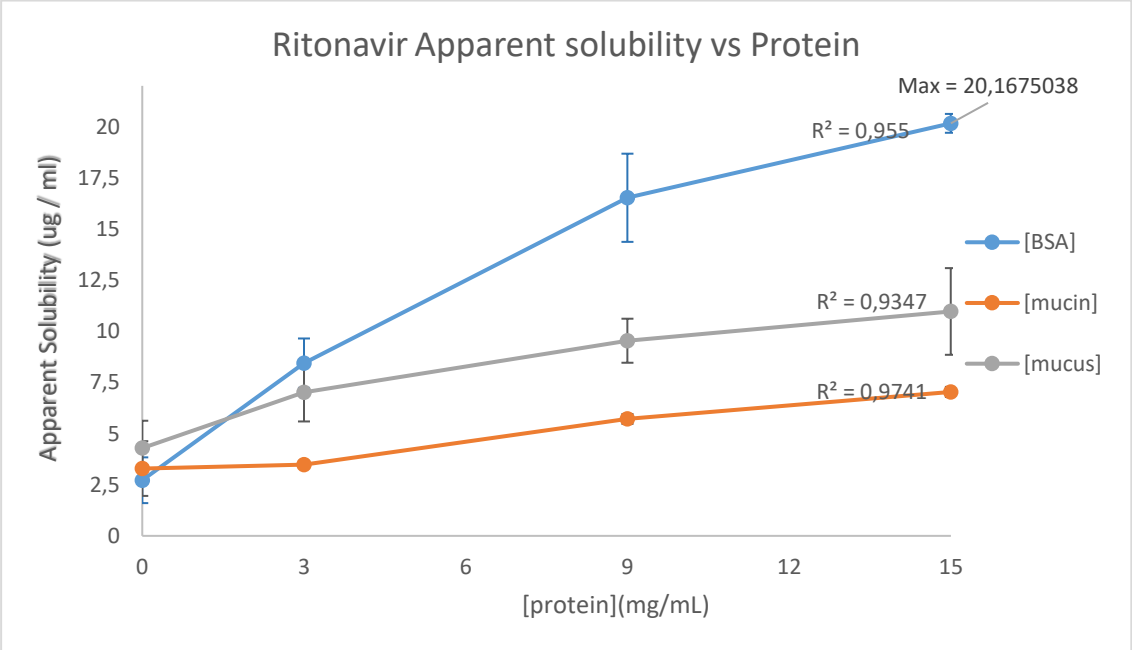

Figure 17: The apparent drug solubility as a function of protein concentration for Ritonavir in FaSSCoF as solvent (n=6). Data shown with ± standard deviation.

5.4 Integration of Results and discussions

The compounds investigated in this thesis shared a common characteristic, they were all small molecules with poor aqueous solubility. These compounds, namely Nilotinib, Carvedilol, and Ritonavir, exhibited an increase in their Apparent solubility when all three protein sources were added to the FaSSCoF media, compared to their individually predicted water solubility. Considering the similarities in the investigated compounds and their solubilization properties, it was observed that no relationship was found among the three compounds in terms of Log P, molecular weight (Mw), BCS class, predicted water solubility, or plasma protein binding.

It could be considerable that pKa values may influence the solubilization properties of poorly soluble compounds. Specifically, the pKa values determine whether the compound becomes ionized or non-ionized in the solubilization solvent [50]. In the case of this study where the pKa values are lower than the pH of FaSSCoF, the compound becomes charged and thus its solubility increases. This implies that mucin and PIM may exhibit similar affinities for ionized drugs such as Nilotinib with pKa_1 3, pKa_2 6 and Ritonavir pKa 2.8 at pH 7.8

All three compounds investigated in this thesis exhibited poor aqueous solubility. It was observed that gastrointestinal fluids, particularly FaSSCoF, possess properties that enhance the apparent drug solubility . Moreover, the addition of three different protein sources to the media further augmented the apparent drug solubility. These findings hold promise for advancing research on new chemical entities and developing colonic drug delivery systems. the comparison between declared water solubility of three compounds and apparent solubility obtained from this study mentioned in table 4.

Despite variations in LogP values, approximately 40% of newly developed comounds demonstrate poor aqueous solubility. LogP determines the compound's Lipophilicity and it is a measure of compound’s differential solubility between hydrophobic and hydrophilic solvents. Poorly soluble and low-absorbed new compunds, as well as known compounds, have exhibited increased variability in bioavailability and toxicity within gastrointestinal mucus. Enhancing bioavailability and solubility is crucial for advancing drug discovery, although it presents a challenge [124].

Table 4: includes the physicochemical properties of the tested compounds. It also presents the known indicated solubility of the compounds in water at 25°C, along with the values of apparent solubility in plain FaSSCoF and the maximum apparent solubility obtained for each compound in this study.

	Nilotinib	**Carvedilol**	**Ritonavir**
MW ($g.mol^{-1}$)	599.5	442.9	720.95
pKa	pKa_1 3 pKa_2 6.2	7.8	2.8
LogP	5.01	3.84	3.9
Plasma protein binding	98.84%	95%	98-99%
Solubility in H2O pH 7 (µg/mL)	2.04	20	0.11
Obtained solubility in FaSSCoF (µg/mL)	0.29	12.45	3.29
Maximum obtained apparent solubility (µg/mL)	3.63	42.35	20.16

6 Conclusion

The aim of this master's thesis was to investigate the impact of proteins present in FaSSCoF (Fasted State Simulated Intestinal Fluid) on compounds exhibiting diverse physicochemical and plasma protein binding properties. The study focused on three compounds namely nilotinib, carvedilol and ritonavir, examining their apparent drug solubility in the presence of three distinct protein sources known as Bovine Serum Albumin (BSA), porcine gastric mucin type II (obtained from dehydrated mucin), and purified intestinal mucus (PIM).

Significant advancements were made in the analytical techniques used to determine the apparent drug solubility in relation to our study. Furthermore, a novel HPLC analysis method was developed for Nilotinib, yielding results comparable to those reported in existing literature, while maintaining the same levels of precision, accuracy, and reproducibility for the prepared FaSSCoF media, as previously demonstrated by other scientists.

The findings of this investigation demonstrated that an increased concentration of all three proteins resulted in a notable increase in the apparent drug solubility within FaSSCoF for all compounds examined. Remarkably, a linear correlation was observed between the elevated protein concentration and the apparent drug solubility for Nilotinib, ritonavir and for carvedilol limited to BSA and Mucin as protein sources.

Additionally, no significant similarities were found in terms of LogP, molecular weight (Mw), Biopharmaceutics Classification System (BCS) class, predicted water solubility, or plasma protein binding. However, the pKa value was observed to potentially influence the solubilization properties of poorly soluble compounds and correlation was identified between the apparent drug solubility of drugs with low PKa value and the utilization of Mucin and PIM as protein sources.

In conclusion, the hypothesis of this thesis, which stated that increasing protein concentration affects the apparent drug solubility of compounds with varying physicochemical properties in FaSSCoF, was confirmed for the three tested drugs.

7 Future Perspective

This thesis aimed to investigate the impact of proteins in FaSSCoF, driven by our interest in enhancing the biorelevance of the media. Additionally, the goal was to develop a more accurate prediction model for protein/peptide concentrations observed in human intestinal fluid (HCF), as reported by Vertzoni et al, which was not considered during the development of the commercial FaSSCoF media [1]. The FaSSCoF media was formulated more than ten years ago, and no subsequent modifications have been made since then. Discrepancies were observed between the apparent drug solubility in the commercial FaSSCoF and the solubility observed in HCF samples obtained from eight fasting individuals. Future research can explore other factors such as enzymes, viscosity, and microorganisms to further improve the biorelevance and complexity of FaSSCoF[1].

Furthermore, this investigation focused on the fasted state, but understanding the influence of proteins in the fed state would also be of great interest.

Improving an apparent drug solubility in the gastrointestinal tract is crucial for predicting overall drug solubility. Acquiring knowledge about the apparent drug solubility in FaSSCoF for compounds with diverse physicochemical properties holds promise for future in silico and computational predictions. In a related study, Fagerberg et al. explored the apparent drug solubility of lipophilic compounds in pH-regulated phosphate buffer, FaSSIF, and human intestinal fluids, aiming to enhance computational modeling for predicting apparent drug solubility[125].

Determining apparent drug solubility can be time-consuming and resource-intensive, particularly in drug discovery where chemical synthesis is often required prior to measurement. Therefore, advancing computational modeling predictions can save time and resources in the discovery of new chemicals. Furthermore, investigating human body fluids poses challenges due to limitations such as donor access and ethical considerations. Fagerberg et al. examined 86 lipophilic compounds and successfully computationally predicted their apparent drug solubility in FaSSIF and human intestinal fluids.

Given the prevalence of numerous newly discovered chemical entities with poor aqueous solubility in recent drug discovery, they represent promising candidates for exploring intestinal and colonic drug delivery systems. Various strategies have been developed to improve the solubility of compounds with limited aqueous solubility. These approaches can be classified into physical and chemical modifications. Physical modifications involve techniques such as reducing particle size, utilizing drug dispersion carriers, and employing cryogenic methods. On the other hand, chemical modifications encompass strategies like adjusting pH, utilizing buffer systems, and employing complexation methods [124] Additionally, descriptive parameters such

as protein-binding properties and pH dependence should be considered to enhance the accuracy of computational modeling, which can be the next step in improving in silico predictions for colonic fluid.

Solubility determination is a time-consuming and resource-intensive process. Moreover, conducting experimental work with meticulous accuracy and precision is essential to obtain validated and reproducible data, which can contribute to reliable in silico predictions of drug absorption. Computational modeling presents an opportunity to achieve similar in silico predictions for colonic drug delivery, while mitigating some of the inherent limitations of in vitro experiments. This approach is particularly essential given the high demand for drug discovery and the exploration of new chemical entities. A computational model was previously developed to predict the behavior of small lipophilic molecules in small intestinal conditions[124]. Therefore, it is realistic to consider further investigations to develop a similar model for colonic conditions. However, a comprehensive investigation encompassing multiple experimental factors is necessary to achieve this goal. Descriptive parameters such as protein-binding properties, fatty acid influence, pH dependence, presence of enzymes, viscosity properties, and bacterial degradation should be considered[1], [33], [45], [126].

These parameters can be integrated into established computational modeling software for physiologically based pharmacokinetic modeling (PBPK) such as GastroPlus® and Simcyp™M, with the aim of enhancing the accuracy and in silico prediction capabilities of colonic fluid compositions [56, 57].

An important parameter for these software tools is the in vivo relevant solubility. It has been observed that the *in vivo* dissolution rate of poorly soluble lipophilic compounds is often underestimated by these models, as they do not adequately account for the solubilization enhancement effects of bile salts and phospholipids, which are more pronounced in highly soluble compounds. Therefore, incorporating apparent drug solubility data in simulated gastrointestinal fluids for both fed and fasted states is crucial to developing reliable PBPK models [127].

Finally, if unlimited time and resources were available in the laboratory, it would be worthwhile to determine the apparent solubility of a broader range of compounds with diverse physicochemical properties. This expanded investigation would provide a more comprehensive understanding of the solubilization behavior and aid in the development of robust in silico predictive models.

8 References

[1] M. Vertzoni *et al.*, "Biorelevant Media to Simulate Fluid in the Ascending Colon of Humans and Their Usefulness in Predicting Intracolonic Drug Solubility," *Pharm Res*, vol. 27, no. 10, pp. 2187–2196, 2010, doi: 10.1007/s11095-010-0223-6.

[2] S. Das, R. Deshmukh, and A. K. Jha, "Role of natural polymers in the development of multiparticulate systems for colon targeting," *Systematic Reviews in Pharmacy*, vol. 1, Jul. 2010, doi: 10.4103/0975-8453.59516.

[3] Y. Han *et al.*, "Multifunctional oral delivery systems for enhanced bioavailability of therapeutic peptides/proteins," *Acta Pharm Sin B*, vol. 9, no. 5, pp. 902–922, 2019, doi: https://doi.org/10.1016/j.apsb.2019.01.004.

[4] N. G. Kotla *et al.*, "Bioresponsive drug delivery systems in intestinal inflammation: State-of-the-art and future perspectives," *Adv Drug Deliv Rev*, vol. 146, pp. 248–266, Jun. 2019, doi: 10.1016/j.addr.2018.06.021.

[5] G. J. Fernandes, L. Kumar, K. Sharma, R. Tunge, and M. Rathnanand, "A Review on Solubility Enhancement of Carvedilol—a BCS Class II Drug," *J Pharm Innov*, vol. 13, no. 3, pp. 197–212, 2018, doi: 10.1007/s12247-018-9319-z.

[6] V. S. Dave, D. Gupta, M. Yu, P. Nguyen, and S. Varghese Gupta, "Current and evolving approaches for improving the oral permeability of BCS Class III or analogous molecules," *Drug Dev Ind Pharm*, vol. 43, no. 2, pp. 177–189, Feb. 2017, doi: 10.1080/03639045.2016.1269122.

[7] A. Y. Abuhelwa, D. B. Williams, R. N. Upton, and D. J. R. Foster, "Food, gastrointestinal pH, and models of oral drug absorption," *European Journal of Pharmaceutics and Biopharmaceutics*, vol. 112, pp. 234–248, 2017, doi: https://doi.org/10.1016/j.ejpb.2016.11.034.

[8] L. Zou, Z. Ni, E. Tsakalozou, and K. M. Giacomini, "Impact of Pharmaceutical Excipients on Oral Drug Absorption: A Focus on Intestinal Drug Transporters," *Clin Pharmacol Ther*, vol. 105, no. 2, pp. 323–325, Feb. 2019, doi: 10.1002/cpt.1292.

[9] P. Kumar and B. Mishra, "Colon Targeted Drug Delivery Systems -An Overview," *Curr Drug Deliv*, vol. 5, pp. 186–198, Jul. 2008, doi: 10.2174/156720108784911712.

[10] C. Wagner, E. Jantratid, F. Kesisoglou, M. Vertzoni, C. Reppas, and J. B. Dressman, "Predicting the oral absorption of a poorly soluble, poorly permeable weak base using biorelevant dissolution and transfer model tests coupled with a physiologically based pharmacokinetic model," *European Journal of Pharmaceutics and Biopharmaceutics*, vol. 82, no. 1, pp. 127–138, 2012, doi: https://doi.org/10.1016/j.ejpb.2012.05.008.

[11] E. Galia, E. Nicolaides, D. Hörter, R. Löbenberg, C. Reppas, and J. B. Dressman, "Evaluation of Various Dissolution Media for Predicting In Vivo Performance of Class I and II Drugs," *Pharm Res*, vol. 15, no. 5, pp. 698–705, 1998, doi: 10.1023/A:1011910801212.

[12] J. B. Dressman, G. L. Amidon, C. Reppas, and V. P. Shah, "Dissolution Testing as a Prognostic Tool for Oral Drug Absorption: Immediate Release Dosage Forms," *Pharm Res*, vol. 15, pp. 11–22, 2004.

[13] J. Dressman, “6. Biorelevant media,” in *Solubility in Pharmaceutical Chemistry*, C. Saal and A. Nair, Eds., Berlin, Boston: De Gruyter, 2020, pp. 149–168. doi: doi:10.1515/9783110559835-006.

[14] B. Greenwood-Van Meerveld, A. C. Johnson, and D. Grundy, “Gastrointestinal Physiology and Function,” *Handb Exp Pharmacol*, vol. 239, p. 1—16, 2017, doi: 10.1007/164_2016_118.

[15] J. Fallingborg, “Intraluminal pH of the human gastrointestinal tract.,” *Dan Med Bull*, vol. 46 3, pp. 183–96, 1999.

[16] E. Thursby and N. Juge, “Introduction to the human gut microbiota,” *Biochemical Journal*, vol. 474, no. 11, pp. 1823–1836, May 2017, doi: 10.1042/BCJ20160510.

[17] S. Jahani, M. Alebouyeh, S. Moghim, H. Amoli, and H. Ghasemian Safaei, “Role of gut microbiota in the pathogenesis of colorectal cancer; A review article,” *Gastroenterol Hepatol Bed Bench*, vol. 11, pp. 101–109, Jul. 2018.

[18] E. F. Enright, B. T. Griffin, C. G. M. Gahan, and S. A. Joyce, “Microbiome-mediated bile acid modification: Role in intestinal drug absorption and metabolism,” *Pharmacol Res*, vol. 133, pp. 170–186, 2018, doi: https://doi.org/10.1016/j.phrs.2018.04.009.

[19] C. D. Klaassen and J. Y. Cui, “Review: Mechanisms of How the Intestinal Microbiota Alters the Effects of Drugs and Bile Acids,” *Drug Metabolism and Disposition*, vol. 43, pp. 1505–1521, 2015.

[20] J. Zhang, J. Zhang, and R. Wang, “Gut microbiota modulates drug pharmacokinetics,” *Drug Metab Rev*, vol. 50, no. 3, pp. 357–368, Jul. 2018, doi: 10.1080/03602532.2018.1497647.

[21] E. Rinninella *et al.*, “What is the Healthy Gut Microbiota Composition? A Changing Ecosystem across Age, Environment, Diet, and Diseases,” *Microorganisms*, vol. 7, no. 1, 2019, doi: 10.3390/microorganisms7010014.

[22] S. Amidon, J. E. Brown, and V. S. Dave, “Colon-Targeted Oral Drug Delivery Systems: Design Trends and Approaches,” *AAPS PharmSciTech*, vol. 16, no. 4, pp. 731–741, 2015, doi: 10.1208/s12249-015-0350-9.

[23] N. Zmora, J. Suez, and E. Elinav, “You are what you eat: diet, health and the gut microbiota,” *Nat Rev Gastroenterol Hepatol*, vol. 16, no. 1, pp. 35–56, 2019, doi: 10.1038/s41575-018-0061-2.

[24] E. Rutayisire, K. Huang, Y. Liu, and F. Tao, “The mode of delivery affects the diversity and colonization pattern of the gut microbiota during the first year of infants’ life: A systematic review,” *BMC Gastroenterol*, vol. 16, Jul. 2016, doi: 10.1186/s12876-016-0498-0.

[25] M. Albouery *et al.*, “Age-Related Changes in the Gut Microbiota Modify Brain Lipid Composition,” *Front Cell Infect Microbiol*, vol. 9, p. 444, 2019, doi: 10.3389/fcimb.2019.00444.

[26] M. Deschasaux *et al.*, “Depicting the composition of gut microbiota in a population with varied ethnic origins but shared geography,” *Nat Med*, vol. 24, no. 10, pp. 1526–1531, 2018, doi: 10.1038/s41591-018-0160-1.

[27] G. Ianiro, H. Tilg, and A. Gasbarrini, “Antibiotics as deep modulators of gut

microbiota: between good and evil," *Gut*, vol. 65, no. 11, pp. 1906–1915, 2016, doi: 10.1136/gutjnl-2016-312297.

[28] X. Zhang, Y. Han, W. Huang, M. Jin, and Z. Gao, "The influence of the gut microbiota on the bioavailability of oral drugs," *Acta Pharm Sin B*, vol. 11, Jul. 2020, doi: 10.1016/j.apsb.2020.09.013.

[29] A. F. Hofmann and L. R. Hagey, "Bile Acids: Chemistry, Pathochemistry, Biology, Pathobiology, and Therapeutics," *Cellular and Molecular Life Sciences*, vol. 65, pp. 2461–2483, 2008.

[30] R. Holm, A. Müllertz, and H. Mu, "Bile salts and their importance for drug absorption," *Int J Pharm*, vol. 453, Jul. 2013, doi: 10.1016/j.ijpharm.2013.04.003.

[31] L. K. Cheng, G. O'Grady, P. Du, J. U. Egbuji, J. A. Windsor, and A. J. Pullan, "Gastrointestinal system," *WIREs Systems Biology and Medicine*, vol. 2, no. 1, pp. 65–79, 2010, doi: https://doi.org/10.1002/wsbm.19.

[32] S. Baliga, S. Muglikar, and R. Kale, "Salivary pH: A diagnostic biomarker," *J Indian Soc Periodontol*, vol. 17, pp. 461–465, Jul. 2013, doi: 10.4103/0972-124X.118317.

[33] A. K. Philip and B. Philip, "Colon targeted drug delivery systems: A review on primary and novel approaches," *Oman Medical Journal*, vol. 25, no. 2. Oman Medical Specialty Board, pp. 70–78, Apr. 01, 2010. doi: 10.5001/omj.2010.24.

[34] I. Geneva, B. Cuzzo, T. Fazili, and W. Javaid, "Normal Body Temperature: A Systematic Review," *Open Forum Infect Dis*, vol. 6, Jul. 2019, doi: 10.1093/ofid/ofz032.

[35] H. J. Gelberg, "Pathophysiological Mechanisms of Gastrointestinal Toxicity☆," *Comprehensive Toxicology*, pp. 139–178, 2017.

[36] M. Herath, S. Hosie, J. Bornstein, A. Franks, and E. Hill-Yardin, "The Role of the Gastrointestinal Mucus System in Intestinal Homeostasis: Implications for Neurological Disorders," *Front Cell Infect Microbiol*, vol. 10, p. 248, Jul. 2020, doi: 10.3389/fcimb.2020.00248.

[37] G. D. Zuidema and C. J. Yeo, *Shackelford's surgery of the alimentary tract*, 5th ed. W.B. Saunders, 2002. Accessed: Jul. 24, 2023. [Online]. Available: https://cir.nii.ac.jp/crid/1130000794511445120.bib?lang=en

[38] R. D. Williams and J. W. Dickey, "Physiology of the colon and rectum," *The American Journal of Surgery*, vol. 117, no. 6, pp. 849–853, 1969, doi: https://doi.org/10.1016/0002-9610(69)90074-9.

[39] N. Cordero and T. H. Wilson, "Comparison of Transport Capacity of Small and Large Intestine," *Gastroenterology*, vol. 41, no. 5, pp. 500–504, 1961, doi: https://doi.org/10.1016/S0016-5085(19)35096-6.

[40] "Challenge and Development Strategy for Colon-Targeted Drug Delivery System," *Pharmaceutical Sciences and Research*, vol. 9, no. 1, May 2022, doi: 10.7454/psr.v9i1.1251.

[41] M. E. V Johansson, J. M. H. Larsson, and G. C. Hansson, "The two mucus layers of colon are organized by the MUC2 mucin, whereas the outer layer is a legislator of

host–microbial interactions," *Proceedings of the National Academy of Sciences*, vol. 108, no. supplement_1, pp. 4659–4665, Mar. 2011, doi: 10.1073/pnas.1006451107.

[42] R. Bansil and B. S. Turner, "The biology of mucus: Composition, synthesis and organization," *Adv Drug Deliv Rev*, vol. 124, pp. 3–15, 2018, doi: https://doi.org/10.1016/j.addr.2017.09.023.

[43] J. E. Vela Ramirez, L. A. Sharpe, and N. A. Peppas, "Current state and challenges in developing oral vaccines," *Adv Drug Deliv Rev*, vol. 114, pp. 116–131, 2017, doi: https://doi.org/10.1016/j.addr.2017.04.008.

[44] M. E. V Johansson, H. Sjövall, and G. C. Hansson, "The gastrointestinal mucus system in health and disease," *Nat Rev Gastroenterol Hepatol*, vol. 10, no. 6, pp. 352–361, 2013, doi: 10.1038/nrgastro.2013.35.

[45] G. Lemmens, A. Van Camp, S. Kourula, T. Vanuytsel, and P. Augustijns, "Drug Disposition in the Lower Gastrointestinal Tract: Targeting and Monitoring," *Pharmaceutics*, vol. 13, p. 161, Jul. 2021, doi: 10.3390/pharmaceutics13020161.

[46] M. Howard, J. Hill, G. Galluppi, and M. Mclean, "Plasma Protein Binding in Drug Discovery and Development," *Comb Chem High Throughput Screen*, vol. 13, pp. 170–187, Feb. 2010, doi: 10.2174/138620710790596745.

[47] M. Drozdzik, I. Czekawy, S. Oswald, and A. Droździk, "Intestinal drug transporters in pathological states: an overview," *Pharmacological Reports*, vol. 72, Jul. 2020, doi: 10.1007/s43440-020-00139-6.

[48] L. McCoubrey, A. Favaron, A. Awad, M. Orlu, S. Gaisford, and A. Basit, "Colonic drug delivery: Formulating the next generation of colon-targeted therapeutics," *J Control Release*, vol. 353, Dec. 2022, doi: 10.1016/j.jconrel.2022.12.029.

[49] "European Pharmacopoeia -2019- General notices Ph.Eur. 9.6".

[50] A. Bauer-Brandl and M. Brandl, "2. Solubility and supersaturation," in *Solubility in Pharmaceutical Chemistry*, De Gruyter, 2019, pp. 27–70. doi: 10.1515/9783110559835-002.

[51] B. J. Boyd *et al.*, "Successful oral delivery of poorly water-soluble drugs both depends on the intraluminal behavior of drugs and of appropriate advanced drug delivery systems," *European Journal of Pharmaceutical Sciences*, vol. 137, p. 104967, 2019, doi: https://doi.org/10.1016/j.ejps.2019.104967.

[52] D. Elder, "1. Solubility – definition and basic physicochemical considerations," in *Solubility in Pharmaceutical Chemistry*, C. Saal and A. Nair, Eds., Berlin, Boston: De Gruyter, 2020, pp. 1–26. doi: doi:10.1515/9783110559835-001.

[53] D. Hörter and J. Dressman, "Influence of physicochemical properties on dissolution of drugs in the gastrointestinal tract," *Adv Drug Deliv Rev*, vol. 46, pp. 75–87, Apr. 2001, doi: 10.1016/S0169-409X(96)00487-5.

[54] E. Jantratid, N. Janssen, C. Reppas, and J. B. Dressman, "Dissolution Media Simulating Conditions in the Proximal Human Gastrointestinal Tract: An Update," *Pharm Res*, vol. 25, no. 7, pp. 1663–1676, Jul. 2008, doi: 10.1007/s11095-008-9569-4.

[55] M. R. C. Marques, R. Loebenberg, and M. Almukainzi, "Simulated biological fluid

with possible application in dissolution testing," *Dissolution Technol*, vol. 18, no. 3, pp. 15–28, 2011.

[56] L. Klumpp, M. Leigh, and J. Dressman, "Dissolution behavior of various drugs in different FaSSIF versions," *European Journal of Pharmaceutical Sciences*, vol. 142, p. 105138, 2020, doi: https://doi.org/10.1016/j.ejps.2019.105138.

[57] L. Klumpp, K. Nagasekar, O. McCullough, A. Seybert, M. Ashtikar, and J. B. Dressman, "Stability of Biorelevant Media Under Various Storage Conditions," *Dissolut Technol*, 2019.

[58] Y. Tsume, D. M. Mudie, P. Langguth, G. E. Amidon, and G. L. Amidon, "The Biopharmaceutics Classification System: Subclasses for in vivo predictive dissolution (IPD) methodology and IVIVC," *European Journal of Pharmaceutical Sciences*, vol. 57, pp. 152–163, 2014, doi: https://doi.org/10.1016/j.ejps.2014.01.009.

[59] A. Dahan, J. M. Miller, and G. L. Amidon, "Prediction of Solubility and Permeability Class Membership: Provisional BCS Classification of the World's Top Oral Drugs," *AAPS J*, vol. 11, no. 4, pp. 740–746, 2009, doi: 10.1208/s12248-009-9144-x.

[60] L. Z. Benet, C. M. Hosey, O. Ursu, and T. I. Oprea, "BDDCS, the Rule of 5 and drugability," *Adv Drug Deliv Rev*, vol. 101, pp. 89–98, 2016, doi: https://doi.org/10.1016/j.addr.2016.05.007.

[61] U.S. Food and Drug Administration, "U S Food and Drug Administration Nilotinib," 2021. Fda.gov (accessed Jul. 25, 2023).

[62] EMA, "Tasigna," *European Medicines Agency*, Sep. 17, 2018. https://www.ema.europa.eu/en/medicines/human/EPAR/tasigna (accessed Jul. 25, 2023).

[63] M. Herbrink, J. H. M. Schellens, J. H. Beijnen, and B. Nuijen, "Improving the solubility of nilotinib through novel spray-dried solid dispersions," *Int J Pharm*, vol. 529, no. 1, pp. 294–302, 2017, doi: https://doi.org/10.1016/j.ijpharm.2017.07.010.

[64] X. Tian *et al.*, "Clinical Pharmacokinetic and Pharmacodynamic Overview of Nilotinib, a Selective Tyrosine Kinase Inhibitor," *The Journal of Clinical Pharmacology*, vol. 58, no. 12, pp. 1533–1540, Dec. 2018, doi: 10.1002/jcph.1312.

[65] A. A. Abu Rmilah, G. Lin, K. H. Begna, P. A. Friedman, and J. Herrmann, "Risk of <scp>QTc</scp> prolongation among cancer patients treated with tyrosine kinase inhibitors," *Int J Cancer*, vol. 147, no. 11, pp. 3160–3167, Dec. 2020, doi: 10.1002/ijc.33119.

[66] K. Gibek, T. Sacha, and K. Cyranka, "Side effects of treatment with tyrosine kinase inhibitors in patients with chronic myeloid leukemia and the occurrence of anxiety symptoms," *Psychiatr Pol*, pp. 1–14, Oct. 2022, doi: 10.12740/PP/OnlineFirst/152782.

[67] N. J. Koehl, R. Holm, M. Kuentz, V. Jannin, and B. T. Griffin, "Exploring the Impact of Surfactant Type and Digestion: Highly Digestible Surfactants Improve Oral Bioavailability of Nilotinib," *Mol Pharm*, vol. 17, no. 9, pp. 3202–3213, Sep. 2020, doi: 10.1021/acs.molpharmaceut.0c00305.

[68] M. Chougule, A. Sirvi, V. Saini, M. Kashyap, and A. T. Sangamwar, "Enhanced biopharmaceutical performance of brick dust molecule nilotinib via stabilized

amorphous nanosuspension using a facile acid–base neutralization approach," *Drug Deliv Transl Res*, Apr. 2023, doi: 10.1007/s13346-023-01334-7.

[69] A. Zakkula, B. B. Gabani, R. K. Jairam, V. Kiran, U. Todmal, and R. Mullangi, "Preparation and optimization of nilotinib self-micro-emulsifying drug delivery systems to enhance oral bioavailability," *Drug Dev Ind Pharm*, vol. 46, no. 3, pp. 498–504, Mar. 2020, doi: 10.1080/03639045.2020.1730398.

[70] H.-L. Lin, L.-C. Chen, W.-T. Cheng, W.-J. Cheng, H.-O. Ho, and M.-T. Sheu, "Preparation and Characterization of a Novel Swellable and Floating Gastroretentive Drug Delivery System (sfGRDDS) for Enhanced Oral Bioavailability of Nilotinib," *Pharmaceutics*, vol. 12, no. 2, p. 137, Feb. 2020, doi: 10.3390/pharmaceutics12020137.

[71] R. R. Ruffolo and G. Z. Feuerstein, "Carvedilol," in *Comprehensive Medicinal Chemistry II*, Elsevier, 2007, pp. 137–147. doi: 10.1016/B0-08-045044-X/00296-0.

[72] S. Singh and C. V Preuss, *Carvedilol*. StatPearls Publishing, Treasure Island (FL), 2022. [Online]. Available: http://europepmc.org/books/NBK534868

[73] M. Packer *et al.*, "The Effect of Carvedilol on Morbidity and Mortality in Patients with Chronic Heart Failure," *New England Journal of Medicine*, vol. 334, no. 21, pp. 1349–1355, May 1996, doi: 10.1056/NEJM199605233342101.

[74] W. H. Frishman, "Carvedilol," *New England Journal of Medicine*, vol. 339, no. 24, pp. 1759–1765, Dec. 1998, doi: 10.1056/NEJM199812103392407.

[75] J. C. Poggi, F. G. Da Silva, E. B. Coelho, M. P. Marques, C. Bertucci, and V. L. Lanchote, "Analysis of carvedilol enantiomers in human plasma using chiral stationary phase column and liquid chromatography with tandem mass spectrometry," *Chirality*, vol. 24, no. 3, pp. 209–214, Mar. 2012, doi: 10.1002/chir.21984.

[76] O. G. Mousa, E. Yousif, and M. H. Al-Mashhadani, "An Overview of Carvedilol Side Effects and it's Importance in Medicine and Industry," *International Journal of Advanced Research in Chemical Science*, vol. 7, pp. 36–41, 2020.

[77] S. Hiendrawan, E. Widjojokusumo, B. Veriansyah, and R. R. Tjandrawinata, "Pharmaceutical Salts of Carvedilol: Polymorphism and Physicochemical Properties," *AAPS PharmSciTech*, vol. 18, no. 4, pp. 1417–1425, May 2017, doi: 10.1208/s12249-016-0616-x.

[78] L. Maggi *et al.*, "Synthesis and Characterization of Carvedilol-Etched Halloysite Nanotubes Composites with Enhanced Drug Solubility and Dissolution Rate," *Molecules*, vol. 28, no. 8, p. 3405, Apr. 2023, doi: 10.3390/molecules28083405.

[79] E.-S. Ha, J.-S. Kim, S.-K. Lee, W.-Y. Sim, J.-S. Jeong, and M.-S. Kim, "Equilibrium solubility and solute-solvent interactions of carvedilol (Form I) in twelve mono solvents and its application for supercritical antisolvent precipitation," *J Mol Liq*, vol. 294, p. 111622, Nov. 2019, doi: 10.1016/j.molliq.2019.111622.

[80] D. Liu *et al.*, "Fabrication of Carvedilol Nanosuspensions Through the Anti-Solvent Precipitation–Ultrasonication Method for the Improvement of Dissolution Rate and Oral Bioavailability," *AAPS PharmSciTech*, vol. 13, no. 1, pp. 295–304, Mar. 2012, doi: 10.1208/s12249-011-9750-7.

[81] S. Eesam, J. S. Bhandaru, C. Naliganti, R. K. Bobbala, and R. R. Akkinepally,

"Solubility enhancement of carvedilol using drug–drug cocrystallization with hydrochlorothiazide," *Futur J Pharm Sci*, vol. 6, no. 1, p. 77, Dec. 2020, doi: 10.1186/s43094-020-00083-5.

[82] N. Bolourchian and M. Shafiee Panah, "The Effect of Surfactant Type and Concentration on Physicochemical Properties of Carvedilol Solid Dispersions Prepared by Wet Milling Method," *Iranian Journal of Pharmaceutical Research*, vol. 21, no. 1, May 2022, doi: 10.5812/ijpr-126913.

[83] M. Krstić *et al.*, "Binary polymeric amorphous carvedilol solid dispersions: In vitro and in vivo characterization," *European Journal of Pharmaceutical Sciences*, vol. 150, p. 105343, Jul. 2020, doi: 10.1016/j.ejps.2020.105343.

[84] T. Loftsson, S. B. Vogensen, C. Desbos, and P. Jansook, "Carvedilol: Solubilization and Cyclodextrin Complexation: A Technical Note," *AAPS PharmSciTech*, vol. 9, no. 2, pp. 425–430, Jun. 2008, doi: 10.1208/s12249-008-9055-7.

[85] S. Sip *et al.*, "Chitosan as Valuable Excipient for Oral and Topical Carvedilol Delivery Systems," *Pharmaceuticals*, vol. 14, no. 8, p. 712, Jul. 2021, doi: 10.3390/ph14080712.

[86] V. Friuli, S. Pisani, B. Conti, G. Bruni, and L. Maggi, "Tablet Formulations of Polymeric Electrospun Fibers for the Controlled Release of Drugs with pH-Dependent Solubility," *Polymers (Basel)*, vol. 14, no. 10, p. 2127, May 2022, doi: 10.3390/polym14102127.

[87] J. E. Choi *et al.*, "Effects of different physicochemical characteristics and supersaturation principle of solidified SNEDDS and surface-modified microspheres on the bioavailability of carvedilol," *Int J Pharm*, vol. 597, p. 120377, Mar. 2021, doi: 10.1016/j.ijpharm.2021.120377.

[88] S. R. Chemburkar *et al.*, "Dealing with the Impact of Ritonavir Polymorphs on the Late Stages of Bulk Drug Process Development," *Org Process Res Dev*, vol. 4, no. 5, pp. 413–417, Sep. 2000, doi: 10.1021/op000023y.

[89] B. Talha and A. S. Dhamoon, *Ritonavir*. StatPearls Publishing, Treasure Island (FL), 2022. [Online]. Available: http://europepmc.org/books/NBK544312

[90] N. I. of D. and D. and K. D. (US), *LiverTox: clinical and research information on drug-induced liver injury*. National Institute of Diabetes and Digestive and Kidney Diseases, 2012. Accessed: Jul. 25, 2023. [Online]. Available: https://www.ncbi.nlm.nih.gov/books/NBK548301/

[91] "ritonavir." go.drugbank.com (accessed Jul. 26, 2023).

[92] EMA(European Medicines Agency), "Norvir," Sep. 17, 2018. https://www.ema.europa.eu/en/medicines/human/EPAR/norvir (accessed Jul. 26, 2023).

[93] R. M. Bonilha Dezena, "Ritonavir Polymorphism: Analytical Chemistry Approach to Problem Solving in the Pharmaceutical Industry," *Brazilian Journal of Analytical Chemistry*, vol. 7, no. 26, 2020, doi: 10.30744/brjac.2179-3425.letter.rmbdezena.N26.

[94] S. L. Morissette, S. Soukasene, D. Levinson, M. J. Cima, and Ö. Almarsson, "Elucidation of crystal form diversity of the HIV protease inhibitor ritonavir by high-

throughput crystallization," *Proceedings of the National Academy of Sciences*, vol. 100, no. 5, pp. 2180–2184, Mar. 2003, doi: 10.1073/pnas.0437744100.

[95] C. Wang *et al.*, "Molecular, Solid-State and Surface Structures of the Conformational Polymorphic Forms of Ritonavir in Relation to their Physicochemical Properties," *Pharm Res*, vol. 38, no. 6, pp. 971–990, Jun. 2021, doi: 10.1007/s11095-021-03048-2.

[96] Selleckchem, "Ritonavir (ABT-538)", Accessed: Apr. 26, 2023. [Online]. Available: https://www.selleckchem.com/datasheet/Ritonavir-S118503-DataSheet.html#s_ref

[97] PubChem (pubchem.ncbi.nlm.nih.gov), "Ritonavir." https://pubchem.ncbi.nlm.nih.gov/compound/ritonavir

[98] K. Hunt, C. A. Hughes, and C. Hills-Nieminen, "Protease Inhibitor–Associated QT Interval Prolongation," *Annals of Pharmacotherapy*, vol. 45, no. 12, pp. 1544–1550, Dec. 2011, doi: 10.1345/aph.1Q422.

[99] medlineplus.gov, "Ritonavir: MedlinePlus Drug Information." https://medlineplus.gov/druginfo/meds/a696029.html (accessed Oct. 22, 2023).

[100] K. R. Shankar, K. P. R. Chowdary, and A. S. Rao, "STUDIES ON ENHANCEMENT OF SOLUBILITY AND DISSOLUTION RATE OF RITONAVIR EMPLOYING β-CYCLODEXTRIN, SOLUPLUS AND PVPK30," *Chowdary et al. World Journal of Pharmaceutical Research World Journal of Pharmaceutical Research SJIF Impact Factor 5*, vol. 4, no. 5, pp. 2614–2624, 2015, [Online]. Available: www.wjpr.net

[101] S. Narala, R. Ampati, and R. Nanam, "Solubility enhancement of ritonavir: Cocrystallization," *J. Pharm. Res*, vol. 8, pp. 630–637, 2019.

[102] K. D. Shah, S. Borhade, and V. Y. Londhe, "UTILIZATION OF CO-CRYSTALLIZATION FOR SOLUBILITY ENHANCEMENT OF A POORLY SOLUBLE ANTIRETROVIRAL DRUG - RITONAVIR," 2014.

[103] T. Velupula *et al.*, "Bioavailability Enhancement of Ritonavir by Solid Dispersion Technique," *Journal of Drug Delivery and Therapeutics*, vol. 11, no. 5, pp. 52–56, 2021.

[104] P. W. Dhore, V. S. Dave, S. D. Saoji, Y. S. Bobde, C. Mack, and N. A. Raut, "Enhancement of the aqueous solubility and permeability of a poorly water soluble drug ritonavir via lyophilized milk-based solid dispersions," *Pharm Dev Technol*, vol. 22, no. 1, pp. 90–102, Jan. 2017, doi: 10.1080/10837450.2016.1193193.

[105] D. Law *et al.*, "Physicochemical considerations in the preparation of amorphous ritonavir–poly(ethylene glycol) 8000 solid dispersions," *J Pharm Sci*, vol. 90, no. 8, pp. 1015–1025, Aug. 2001, doi: 10.1002/jps.1054.

[106] W. J. Lough and I. W. Wainer, *High performance liquid chromatography: fundamental principles and practice*. cRc press, 1995.

[107] D. C. Harris, *Quantitative chemical analysis*. Macmillan, 2010. Accessed: Jul. 25, 2023. [Online]. Available: http://orbitals.ir/wp-content/uploads/2017/01/Daniel-C.-Harris-Quantitative-Chemical-Analysis-8th-Edition-W.-H.-Freeman-2010-Www.Orbitals.ir_.pdf

[108] J. P. Hutchinson, G. W. Dicinoski, and P. R. Haddad, "Aerosol-Based Detectors in

Liquid Chromatography: Approaches Toward Universal Detection and to Global Analysis," *Charged Aerosol Detection for Liquid Chromatography and Related Separation Techniques*, pp. 191–219, 2017.

[109] M. Yuki *et al.*, "High-Performance Liquid Chromatographic Assay for the Determination of Nilotinib in Human Plasma," *Biol Pharm Bull*, vol. 34, no. 7, pp. 1126–1128, 2011, doi: 10.1248/bpb.34.1126.

[110] S. Choudhury, A. Hossain, D. Kundu, T. Sharmin, and M. Maleque, "A SIMPLE REVERSED PHASE HIGH PERFORMANCE LIQUID CHROMATOGRAPHY METHOD DEVELOPMENT AND VALIDATION FOR DETERMINATION OF CARVEDILOL IN PHARMACEUTICAL DOSAGE FORMS," *International Journal of Advances in Pharmaceutical Analysis*, Jun. 2013.

[111] N. Hokama, N. Hobara, H. Kameya, S. Ohshiro, and M. Sakanashi, "Rapid and simple micro-determination of carvedilol in rat plasma by high-performance liquid chromatography," *J Chromatogr B Biomed Sci Appl*, vol. 732, no. 1, pp. 233–238, Sep. 1999, doi: 10.1016/S0378-4347(99)00248-0.

[112] M. Machida, M. Watanabe, S. Takechi, S. Kakinoki, and A. Nomura, "Measurement of carvedilol in plasma by high-performance liquid chromatography with electrochemical detection," *Journal of Chromatography B*, vol. 798, no. 2, pp. 187–191, Dec. 2003, doi: 10.1016/j.jchromb.2003.09.039.

[113] J. Oravcova, D. Sojkova, and W. Lindner, "Comparison of the Hummel—Dreyer method in high-performance liquid chromatography and capillary electrophoresis conditions for study of the interaction of (RS)-, (R)- and (S)-carvedilol with isolated plasma proteins," *J Chromatogr B Biomed Sci Appl*, vol. 682, no. 2, pp. 349–357, Jul. 1996, doi: 10.1016/0378-4347(96)00092-8.

[114] M. Sultan, "Simultaneous determination of carvedilol and hydrochlorothiazide in tablets by derivative spectrophotometric and HPLC methods," *Asian Journal of Chemistry*, vol. 20, pp. 2283–2292, Mar. 2008.

[115] C. L. Dias, A. M. Bergold, and P. E. Fröehlich, "UV-Derivative Spectrophotometric Determination of Ritonavir Capsules and Comparison with LC Method," *Anal Lett*, vol. 42, no. 12, pp. 1900–1910, Jul. 2009, doi: 10.1080/00032710903060701.

[116] C. Dias, R. Rossi, E. M. Donato, A. Bergold, and P. E. Fröehlich, "LC Determination of Ritonavir, a HIV Protease Inhibitor, in Soft Gelatin Capsules," *Chromatographia*, vol. 62, pp. 589–593, Dec. 2005, doi: 10.1365/s10337-005-0670-0.

[117] R. M. W. Hoetelmans, M. van Essenberg, M. Profijt, P. L. Meenhorst, J. W. Mulder, and J. H. Beijnen, "High-performance liquid chromatographic determination of ritonavir in human plasma, cerebrospinal fluid and saliva," *J Chromatogr B Biomed Sci Appl*, vol. 705, no. 1, pp. 119–126, Jan. 1998, doi: 10.1016/S0378-4347(97)00500-8.

[118] A. V Sulebhavikar, U. D. Pawar, K. V Mangoankar, and N. D. Prabhu-Navelkar, "HPTLC Method for Simultaneous Determination of Lopinavir and Ritonavir in Capsule Dosage Form," *E-Journal of Chemistry*, vol. 5, p. 539849, 2008, doi: 10.1155/2008/539849.

[119] M. Musuluri, "A RP-HPLC method for the estimation of Ritonavir in pharmaceutical dosage forms," *J Pharm Res*, vol. 4, p. 3049, Dec. 2011.

[120] M. S. Imam, A. S. Batubara, M. Gamal, A. H. Abdelazim, A. A. Almrasy, and S. Ramzy, “Adjusted green HPLC determination of nirmatrelvir and ritonavir in the new FDA approved co-packaged pharmaceutical dosage using supported computational calculations,” *Sci Rep*, vol. 13, no. 1, p. 137, Jan. 2023, doi: 10.1038/s41598-022-26944-y.

[121] H. K. Pabolu and S. K. Konidala, “New validated RP-HPLC method for the determination of ritonavir in bulk and pharmaceutical dosage form,” *Int J Pharm Pharm Sci*, vol. 5, pp. 556–559, 2013.

[122] M. Khoder, H. Abdelkader, A. ElShaer, A. Karam, M. Najlah, and R. G. Alany, “Efficient approach to enhance drug solubility by particle engineering of bovine serum albumin,” *Int J Pharm*, vol. 515, no. 1–2, pp. 740–748, Dec. 2016, doi: 10.1016/j.ijpharm.2016.11.019.

[123] X. Cai *et al.*, “Addition of Optimized Bovine Serum Albumin Level in a High-Throughput Caco-2 Assay Enabled Accurate Permeability Assessment for Lipophilic Compounds,” *SLAS Discovery*, vol. 24, no. 7, pp. 738–744, Aug. 2019, doi: 10.1177/2472555219848483.

[124] K. T. Savjani, A. K. Gajjar, and J. K. Savjani, “Drug Solubility: Importance and Enhancement Techniques,” *ISRN Pharm*, vol. 2012, pp. 1–10, Jul. 2012, doi: 10.5402/2012/195727.

[125] J. H. Fagerberg, E. Karlsson, J. Ulander, G. Hanisch, and C. A. S. Bergström, “Computational Prediction of Drug Solubility in Fasted Simulated and Aspirated Human Intestinal Fluid,” *Pharm Res*, vol. 32, no. 2, pp. 578–589, Feb. 2015, doi: 10.1007/s11095-014-1487-z.

[126] M. V. Calvo and A. Dominguez-Gil, “Binding of naproxen to human albumin. Interaction with palmitic acid,” *Int J Pharm*, vol. 16, no. 2, pp. 215–223, Sep. 1983, doi: 10.1016/0378-5173(83)90058-3.

[127] H. Jones and K. Rowland-Yeo, “Basic Concepts in Physiologically Based Pharmacokinetic Modeling in Drug Discovery and Development,” *CPT Pharmacometrics Syst Pharmacol*, vol. 2, no. 8, p. 63, Aug. 2013, doi: 10.1038/psp.2013.41.

Appendix
Appendix A

RP-HPLC-UV method for Nilotinib:

Column: C18 100 mm x 4.6 mm, 5 µm

Column temperature: 40°C

Organic phase: ACN

Aquarius phase: 1.36 g/L solution of potassium dihydrogen phosphate-buffered solution (pH = 2), adjusted with phosphoric acid

Eluent time: 19 min

Flow rate: 0.800

Injection volume: 10µL

UV-length detection: 240nm

Retention time (R_T): 12-13 min

Method inspired from: European Pharmacopoeia [Ph. Eur.9th Eddition.]

Table 5: RP-HPLC-UV method for nilotinib with isocratic flow

Time [min]	Flow rate [mL/min]	% Aquarius Phase	% Organic Phase
0.000	0.800	90.0	10.0
2.000	0.800	90.0	10.0
16.000	0.800	10.0	90.0
17.000	0.800	10.0	90.0
18.000	0.800	90.0	10.0
19.000	0.800	90.0	10.0

RP-HPLC-UV method for Carvedilol:

Column: C18 150 mm x 4.6 mm, 5 µm

Column temperature: 25°C

Organic phase: 0.1% TFA in ACN

Aquarius phase: 10 mmol/L sodium phosphate solution (pH 2)

Eluent time: 5 min

Flow rate: 1.000

Injection volume: 10 µL

UV-length detection: 210 nm

Retention time (R_T): 2.75 ± 0.03

Method inspired from [114]

Table 6: RP-HPLC-UV method for carvedilol with isocratic flow.

Time [min]	Flow rate [mL/min]	% Aquarius Phase	% Organic Phase
0.000	1.000	60.0	40.0
5.000	1.000	60.0	40.0

RP-HPLC-UV method for Ritonavir:

Column: C18 100 mm x 4.6 mm, 5 µm

Column temperature: 30°C

Organic phase: ACN

Aquarius phase: MQ water

Eluent time: 9 min

Flow rate: 0.800

Injection volume: 10µL

UV-length detection: 210nm

Retention time (R_T): 7.2-7.4 min

Method inspired from [121].

Table 7: RP-HPLC-UV method for Ritonavir with isocratic flow.

Time [min]	Flow rate [mL/min]	% Aquarius Phase	% Organic Phase
0.000	0.800	60.0	40.0
1.000	0.800	60.0	40.0
8.000	0.800	20.0	80.0
8.500	0.800	20.0	80.0
9.000	0.800	60.0	40.0

Appendix B

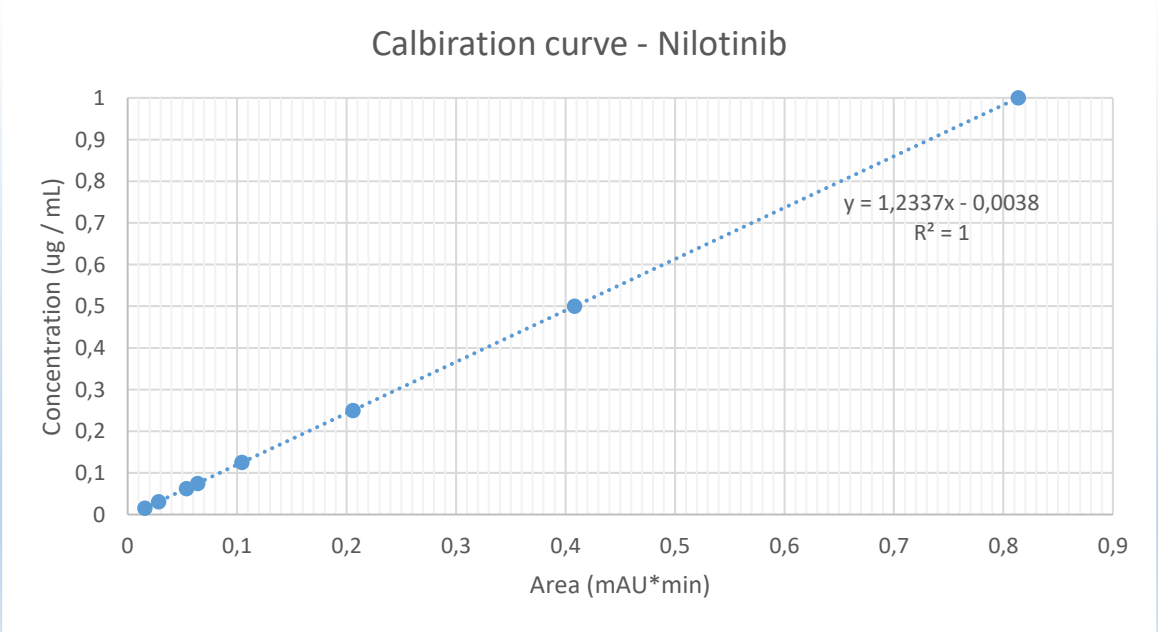

Figure 18: The HPLC Calibration curve of Nilotinib. Illustrates concentration of standards as a function of obtained area.

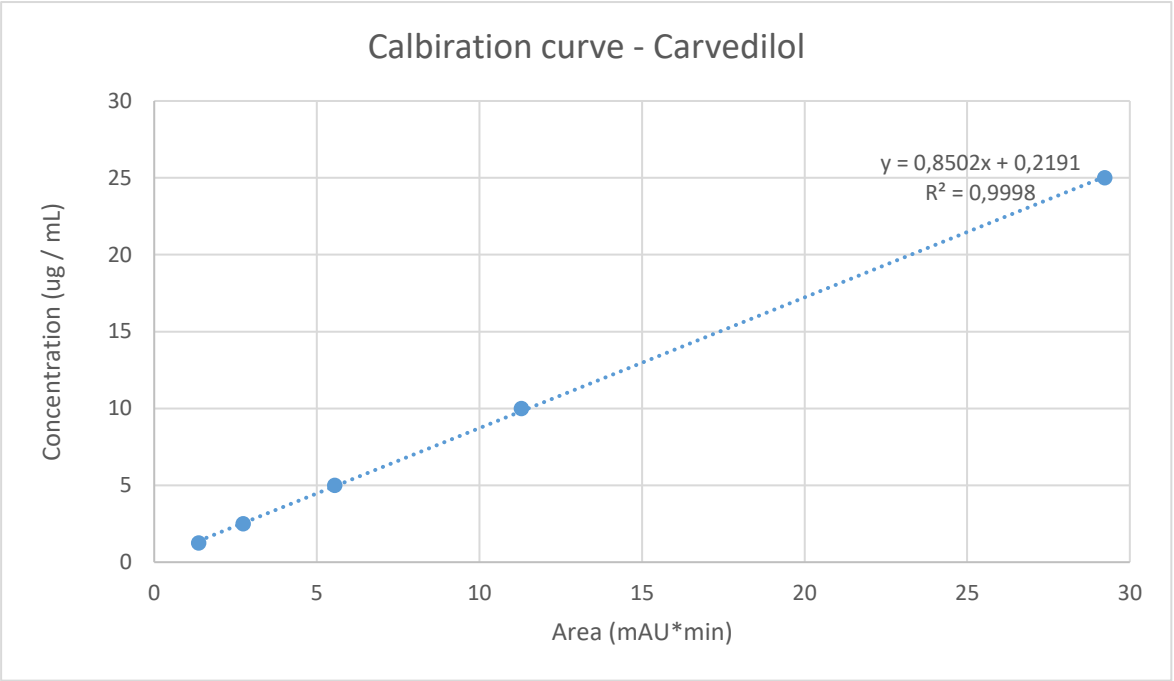

Figure 19: The HPLC Calibration curve of Carvedilol. Illustrates concentration of standards as a function of obtained area.

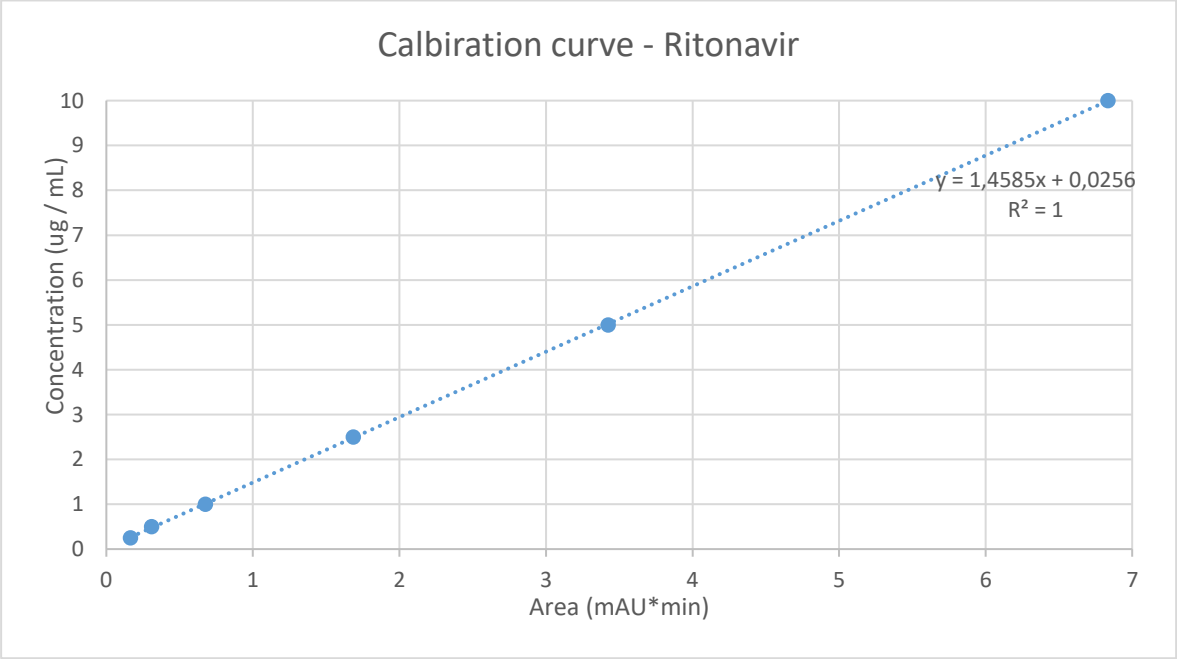

Figure 20: The HPLC Calibration curve of Ritonavir. illustrates concentration of standards as a function of obtained area.

Appendix C

Table 8: Slopes and R^2 of simple linear regression for the Apparent Solubility over protein concentration for the protein sources of BSA, Mucin, PIM.

Compound	BSA	Mucin	PIM
Nilotinib	y = 0.0427x + 0.2346 R^2 = 0.9781	y = 0.0104x + 0.1809 R^2 = 0.961	y = 0.2364x + 0.2657 R^2 = 0.9757
Carvedilol	y = 2.0309x + 12.21 R^2 = 0.9977	y = 0.7308x + 12.013 R^2 = 0.9795	y = 0.85x + 17.158 R^2 = 0.6374
Ritonavir	y = 1.1567x + 4.1565 R^2 = 0.955	y = 0.2683x + 3.0713 R^2 = 0.9741	y = 0.4272x + 5.0699 R^2 = 0.9347